Anton Xu, BSc.

Development of an in-vitro 3D reconstructed human epidermal skin model with in-vivo like barrier function

MASTER'S THESIS

to achieve the university degree of

Master of science

Master's degree programme: Molecular Microbiology

Submitted to

Graz University of Technology

Supervisor

Univ-Prof. mag. Dr. rer.nat. Joachim REIDL

Institute of Molecular Bioscience

Graz, October 2016

Affidavit

I declare that I have authored this thesis independently, that I have not used other than the declared sources/resources, and that I have explicitly indicated all material which has been quoted either literally or by content from the sources used. The text document uploaded to TUGRAZonline is identical to the present master‘s thesis.

Graz, October 2016 .....

Acknowledgment

First of all I would like to thank my thesis supervisor Dr. Florian Groeber and Prof. Dr. Heike Walles of Fraunhofer Institute of Interfacial Engineering and Biotechnology and Prof. Dr. Joachim Reidl of Karl-Franzens University of Graz for giving me this opportunity to work on my thesis at the Chair of Tissue Engineering and Regenerative Medicine, Würzburg. Dr. Groeber entrusted me with the freedom to establishing thesis as my own work but provided me with guidance in the right direction whenever I had troubles or was straying off the path.

I would also like to thank Freia Schmid, MSc. for her inexhaustible patience, help and guidance during my work and as the second reader of this thesis. I am gratefully indebted to her for her valuable and relentless comments on this thesis.

Finally I must express my very profound gratitude to my parents for providing me with unfailing support and continuous encouragement throughout my years of study and through the process of researching and writing this thesis. This accomplishment would not have been possible without them. Thank you.

Author

Anton Xu

Kurzfassung

Die Haut kommt als äußerste Barriere des Menschen im Alltag mit chemischen Substanzen verschiedenster Natur in Kontakt über deren Risiken und Gefahren man dank der Forschung und ihren Tierversuchen Bescheid weiß. Fortschritte im Bereich *Tissue Engineering* erlauben es das Tierversuchsmodelle zunehmend von in-vitro Hautmodellen ersetzt werden. Diese haben sowohl moralische als auch praktische Vorteile, denn dadurch repräsentieren Experimente menschliche Zellen und deren Reaktionen anstatt die der Versuchstiere. Bisher wurde jedoch berichtet dass die Barrierefunktion von in-vitro Hautmodellen nicht an den natürlichen Wert herankommt. Sehr problematisch stellt dieser Umstand sich bei Experimenten heraus die auf die Penetration von Substanzen testen. Das Ziel dieser Arbeit war die Barrierefunktion durch Modifikationen im derzeitigen Protokoll für Hautmodelle zu erhöhen um ein Niveau zu erreichen, welches mit der natürlichen menschlichen Haut vergleichbar ist.

Für diese Fragestellung wurden mehrere Lösungsansätze aus der Literatur abgeleitet, eine Behandlung der Hautmodelloberfläche mit Glykolsäure, die Supplementation von Lipiden im Medium und die Besiedlung des Hautmodells durch den kommensalen *Staphylococcus epidermidis*. Die Supplementation von diversen Lipiden zeigte am meisten Potential nach ersten Versuchen und wurde daher für weitere Untersuchungen benutzt. Durch verschiedene Charakterisierungsmethoden wie die Immunhistologie, Impedanzspektroskopie, Ramanspektroskopie und der Messung von transepidermalem Wasserverlust konnte der Hintergrund, der durch die Lipidsupplementation beobachteten Erhöhung der Barriere, besser analysiert werden. Das Ergebnis zeigte sich bei irritativen Substanztestungen und transepidermalen Wasserverlust positiv während bei die Methoden Impedanzspektroskopie und Ramanspektroskopie keine signifikanten Verbesserungen interpretiert wurden.

Abstract

The skin is the outermost boundary between the human body and the environment including the abundance of chemical substances which the skin comes into contact with in everyday life. Most risks and hazards of these substances have been identified through research and animal testing. Advancements in tissue engineering have enabled the culture of in-vitro skin models, a more moral and practical way of conducting safety research. Looking to replace animal testing, it benefits additionally as results are more representative of the native human skin. However recent studies report a deficient barrier function within these skin models when compared to the native human skin. This is particularly problematic when testing substances for skin adsorption. The aim of this thesis is to improve the barrier function of in-vitro skin models by modifying the current protocol to approximate levels comparable to native human skin. The aim of this thesis is to develop methods to generate an *in-vitro* reconstructed human epidermis with an improved barrier function.

Using literature multiple approaches were drafted and tested during an initial round of testing. These approaches include the topical application of glycolic acid, the supplementation of lipid species and the introduction of a skin commensal, *Staphylococcus epidermidis*. Based on the results and the highest potential the lipid supplementation was chosen for further characterization using various methods such as immunohistochemistry, impedance spectroscopy, raman spectroscopy and transepidermal waterloss measurements. While the analysis of the results indicated an improved barrier function for irritative substance test and transepidermal waterloss measurements, impedance spectroscopy and raman spectroscopy showed results which implied no significant changes.

Table of contents

1. Introduction

1.1 Human skin and the barrier function

1.1.1 Anatomy of the human skin

The skin is the largest organ of the human body and plays a pivotal role protecting the body from harsh environmental conditions [1]. As the outermost layer, it is subjected to constant exogenous hazards, including UV-irradiation, pathogens, mechanical and chemical stress while simultaneously preventing loss of endogenous water, ions and nutrients [2].The importance of the human skin barrier is well illustrated in situations where a deficient barrier function, such as in premature infants or severe thermal burns resulting in dehydration and serum electrolyte alteration [3]. A healthy human skin consists of three major layers. It is separated into the innermost subcutis, the overlaying dermis and the epidermis (see Fig. 1). The dermis is composed of adipocytes, fibroblasts, macrophages and connective tissue, prevents the loss of body heat and stores triglycerides as energy reserves. The epidermis is a stratified tissue which contains layers of keratinocytes in various stages of differentiation.

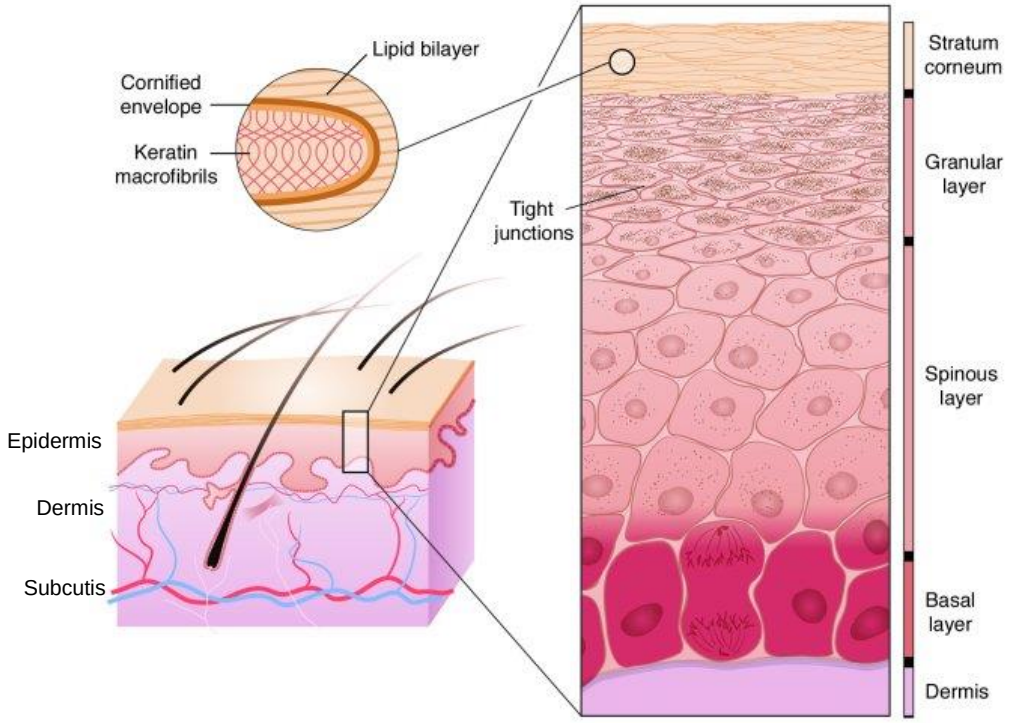

Figure 1: Anatomy of the human skin including layers of keratinocyte differentiation stages and the composition of the stratum corneum. Image source: Segre et al, J. Clin. Invest. 2006

The four layers of the epidermis are designated as *stratum basale* (SB) bordering the dermis, *stratum spinosum* (SS), *stratum granulosum* (SG) and lastly the surfacing *stratum corneum* (SC). SB, SS and SG are referred to as the viable epidermis while SC is referred to as the non-viable epidermis. Around 80% of the epidermal cells are human epidermal keratinocytes (HEK) which follow a successive differentiation program during migration from proliferation in SB until eventual desquamation in SC [4]. HEK in the SG form distinctive granules containing lipids and enzymes responsible for the formation and maintenance of the cornified envelope (CE) of the SC [5]. On the outermost section, the approximately 20 µm thick SC is often described as a brick-and-mortar structure [6]. In this case, the bricks are corneocytes which terminally differentiate to flattened cells filled with keratin and devoid of nuclei and other cytoplasmic organelles. Together with the mortar component which is comprised of ceramides, cholesterol and fatty acids, the lipid-protein matrix of the SC provides the main barrier against water loss and external hazards [7].

1.1.2 Lipid metabolism and presence in the stratum corneum

As mentioned above the SC, the outermost boundary of the human body, consists of corneocytes covered in a neutral lipid enriched extracellular matrix to form the permeability barrier and antimicrobial barrier [5]. Studies have shown that this lipid matrix accounts for approximately 10% of the SC's tissue mass. It's approximate composition was also reconfirmed by various different research groups to be 50% lipid mass ceramides, 25% cholesterol and 15% free fatty acids with very little phospholipid [5], [8], [9]. These lipids are transported together with processing enzymes by lamellar bodies and released into the SC (see Fig. 2). Lamellar bodies are ovoid, 0.2 x 0.3 µm membrane bilayer-encircled secretory organelles which are first formed during keratinocytes differentiation in the SS and particularly visible in the SG due to sheer numbers [10]. Once released from the lamellar bodies, the lipids are modified by co-secreted enzymes. Phospholipids are converted into free fatty acids (FFA) and glycerol by phospholipase A2 [11], [12]. While ceramides are generated by at least two different enzymes both the acidic sphingomyelinase and the beta-glucocerebrosidase from sphingomyelin and glucosylceramides respectively [13], [14]. It is suggested that the proper supplementation of lipids is imperative for CE formation and barrier function [5]. In this thesis, it is hypothesized that the absence of the dermis and therefore the missing supplementation of non-essential fatty acid creates a bottleneck which impairs the proper synthesis of functional lipids within lamellar bodies. As a consequence this effect would also cause proper formation and maintenance of the SC's barrier function.

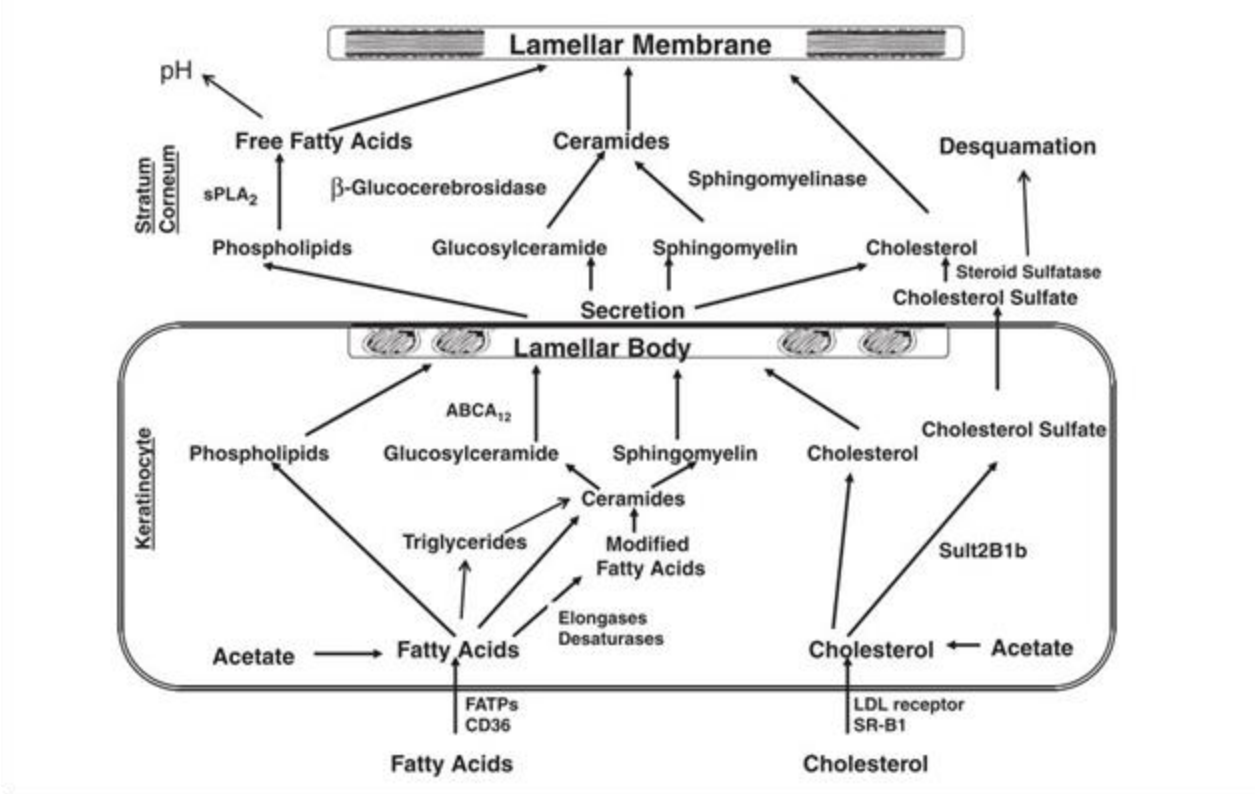

Figure 2: Pathways for the formation of lamellar bodies which contribute to the stratum corneum's barrier formation and maintenance. Image Source: Elias et al 2014

1.1.3 Microbial skin flora

Native human skin does possess an extensive biome of commensal microbes which have been largely disregarded for testing purposes. It is suggested that microbes contributed to a large extent to the barrier function by metabolizing human secretions such as sweat or sebum [15], [16]. It is reported in literature that the surface of the healthy human skin possesses an acidic pH in the range of 4.0-7.0 whereas surface pH below a pH of 5.0 is known for better barrier function [3], [17]. This acid mantle and the concomitant pH gradient within the SC are also very important for residential microbes such as *Staphylococcus epidermidis* [17]. This symbiotic relationship allows microbes to colonize up to 80% of the human skin surface in exchange for contributions against other potential pathogenic agents but also further acidification of the SC [18], [19]. This particular aspect of a co-existent microbial skin flora has not been considered within current standard protocols for skin models under the standard sterile conditions for cell biology and tissue engineering.

1.2 Alternatives to animal models

Traditionally animal experiments have always been used to assess unknown hazardous potentials of chemical substances despite species specific differences in anatomy and metabolism [20], [21]. While this was necessary due to the lack of reliable alternative options, animal testing has always, since the 1950s, been working on principles which were termed “the three Rs” [22]. These “Rs” stand for reduction, strategies to minimize the number of subjects necessary to obtain sufficient data or the maximizing of data per animal subject, refinement, the modification of experimental procedures to reduce suffering and increase overall life quality of animals used, and lastly replacement. There is relative replacement which means using animals of lower potential for pain reception according to current scientific knowledge such as invertebrates instead of more sentient animals and absolute replacement implying the use of computer models or testing done on inanimate or in-vitro systems [22]. A step in this direction and away from animal testing would be more ethical, less resource intensive and aims to be vastly more accurate than animal models.

1.2.1 Regulatory acceptance and ECVAM

Since it became operational in 1993 the European Centre for the Validation of Alternative Methods (ECVAM) as part of the European Commission’s Joint Research Centre, its main objective is to validate alternative methods in regards to European Union (EU) standards and regulations which aim at the “Three Rs” principles as mentioned above. After extensive discussions and a failure to impose a testing ban on the 6th amendment of the cosmetic directive, the European Parliament and Council introduced the 7th amendment to the cosmetic directive 76/768/EEC in March 2003, a regulatory framework set to phase out animal testing for cosmetic purposes. This directive specified a timeframe for testing and marketing ban on products which were tested on animals [23], [24]. Furthermore, in 2006 a new regulative initiative came into effect on the Regulation, Evaluation, Authorization and Restriction of Chemicals (REACH) by the EU in regards to the use of chemicals and their safety [25]. The regulation required all companies manufacturing and importing chemicals into the EU in

quantities exceeding 1 ton per year to submit a registration dossier with possible adverse effects on the environment or human health to the European Chemicals Agency [26]. While largely welcomed this would also imply the necessity of risk and safety assessments using animal testing, increasing the demand up to 45 million laboratory animals over the next 15 years [27]. In response to these challenges ECVAM cooperated with the Organisation for Economic Co-operation and Development (OECD) to incorporate existing testing guidelines into the directive as alternate testing method. These included OECD test guideline (TG) 430 and 431 for skin corrosion and later OECD TG 439 for skin irritation [23]. Since then, commercially available skin models have been developed and accepted for dermatologic research in areas by validating through these OECD test guidelines [28]–[30].

1.2.2 Reconstructed human epidermis model

It was at the advent of improved cultures and maturation of keratinocytes by exposure to an air-liquid interface (ALI) that has led to the possibility of the reconstruction of realistic cultured epidermis [31]. The regulations and laws imposed on the cosmetic industry as mentioned above prompted rising demands on alternatives to animal testing [24]. Over time, various research groups identified and contributed important factors such as cell density, keratinocyte isolation and protein expression to further expand possibilities and understanding of this technique [32]–[34]. Until today, various *in-vitro* skin models ranging from full thickness skin models which also include the dermal layer to epidermis-only models have been developed. The reconstructed human epidermis (RHE) consists of a multilayer of differentiating HEKs grown on an acellular matrix. An ALI culture phase facilitates the development of a cornified SC [31], [35]. While current protocol do achieve the differentiation and formation of all epidermal layers there are still some parameters of the skin models are critically lacking. One area in particular is the barrier function of RHE which shows an increased permeability in contrast to native human SC [36]. This is problematic for the standardization of substance tests involving skin adsorption as parameters are not representative of native human skin. Current research groups are mainly focused on the responsible part of the epidermis for the barrier function such as

the lipid composition of the SC and the enzymatic system which regulates, produces and processes said lipids [37], [38]. There are also other possible causes considered such as the air humidity during cell culture or the calcium homeostasis within the epidermis [39]–[41].

1.3 Aim of the thesis

Based on the work of *Poumay et al* the culture of an *in-vitro* RHE including all distinctive differentiation layers of the native skin is possible [31]. However, publications show, a deficiency within the physical properties of the RHE barrier function [36]. Thus, in vitro models show a higher flux of various test substances compared to the native human skin that is particularly problematic for skin adsorption. The aim of this thesis is to develop methods to generate *in-vitro* RHE with an improved barrier function.

To achieve this, different strategies to modify and improve an existing protocol to generate RHE were tested. Each approach focused on a property of the native skin that is not yet addressed within the current protocol. Factors such as lipid distribution and abundance ratio, pH and calcium gradient within the SC have been reported as important contributors for a physiological barrier function. The focus of this study is to improve lipid supplementation during culture to approximate the presence of lipid species and their ratio to native tissue. Furthermore, strategies are explored to enable the introduction of microbial skin commensals as they represent an additional and influential part of the human skin. For this thesis a common human skin commensal, *staphylococcus epidermidis*, was chosen to pilot the colonization of an RHE skin model. Moreover, as there is a lack of predictive readouts to quantify the RHE barrier, new measuring tools were developed. Multiple techniques have been used to measure different aspects of barrier functionality within the phenotypes derived from each protocol which include transepidermal water loss, an indicator of physical barrier function and measured with the TEWAmeter® TM 300 (Courage Khazaka), marker enzymes that are known precursors of barrier-function contributing mechanisms [37] and resistance against irritative conditions via 3-

(4,5-Dimethylthiazol-2-yl)-2,5diphenyltetrazolium bromide (MTT) cell viability assays.

2. Material and methods

2.1 Chemicals, Media and Solutions

Table 1: Used chemicals

Chemical/Solution	Producer	Catalog No
3-(4,5-Dimethylthiazol-2-yl)-2,5diphenyltetrazolium bromide (MTT)	Serva, Heidelberg (GER)	20395.04
4',6-Diamidino-2-phenylindole dihydrochloride (DAPI)	Sigma-Aldrich, Munich (GER)	D9542-10MG
Accutase	Life technologies, Darmstadt (GER)	A11105-01
Acetic acid	Sigma-Aldrich, Munich (GER)	A6283-2.5L
Acetone, ≥99.5 %	Carl Roth, Karlsruhe (GER)	5025.5
Agarose	Sigma-Aldrich, Munich (GER)	A9539-500G
Antibody diluent DCS	Innovative Diagnostik-Systeme, Hamburg (GER)	AL120R500
Calcium chloride dihydrate ($CaCl_2$*$2H_2O$)	Sigma-Aldrich, Munich (GER)	C7902-500G
Citric acid	Sigma-Aldrich, Munich (GER)	C07599-5KG
Descosept	Dr. Schumacher, Malsfeld (GER)	00311L-100
Dimethyl sulfoxide (DMSO)	Sigma-Aldrich, Munich (GER)	D8418
Dispase II powder	Life technologies, Darmstadt (GER)	17105-041
Eosin	Sigma-Aldrich, Munich (GER)	861006-25G
EpiLife®	Life technologies, Darmstadt (GER)	M-EPI-500-CA
Ethanol 96 %, denatured	Carl Roth, Karlsruhe (GER)	T171.4
Ethanol, absolute	Carl Roth, Karlsruhe (GER)	9065.4
Ethylenediaminetetaacetic acid (EDTA)	Sigma-Aldrich, Munich (GER)	E5134-1kg
Fetal Calf Serum (FCS)	Bio&SELL, Feucht (GER)	FCS.ADD.0500
Glutaraldehyde solution, 25 % in H_2O	Sigma-Aldrich, Munich (GER)	G5882-100ML
Glycolic acid	Sigma-Aldrich, Munich (GER)	420581
Haematoxylin	Carl Roth, Karlsruhe (GER)	3861.1
HEPES	Sigma-Aldrich, Munich (GER)	H4034-10G
Human keratinocyte growth supplement (HKGS), 100x	Life technologies, Darmstadt (GER)	S-001-5
Hydrochloric acid (HCl, 37 %, 1 M)	Carl Roth, Karlsruhe (GER)	1090571000
isopropanol	Sigma-Aldrich, Munich (GER)	33539-2.5L-GL-R
Keratinocyte growth factor (KGF)	Sigma-Aldrich, Munich (GER)	K1757-10UG
L-ascorbyl-2-phosphate	Sigma-Aldrich, Munich (GER)	A8960

Lipid mixture 1	Sigma-Aldrich, Munich (GER)	L0288-100ML
Mounting medium: Entellan	Merck, Darmstadt (GER)	1.079-600.500
Mowiol 4-88	Sigma-Aldrich, Munich (GER)	81381-250G
O.C.T.™ Compound	Sakura, Alphen aan den Rijn (NL)	4583
Paraffin	Carl Roth, Karlsruhe (GER)	6642.6
Penicillin / Streptomycin	Sigma-Aldrich, Munich (GER)	P4333-100ML
Phosphate-buffered saline with calcium and magnesium (PBS^+)	Sigma-Aldrich, Munich (GER)	D8662
Phosphate-Buffered Saline without calcium and magnesium (PBS^-)	Sigma-Aldrich, Munich (GER)	D8537
Roti®-Histofix 4 %	Carl Roth, Karlsruhe (GER)	P087.5
Sodium hydroxyde (NaOH) pellets	Sigma-Aldrich, Munich (GER)	30620-1KG-R
Triton X-100	Sigma-Aldrich, Munich (GER)	T8787
Trypan Blue, 0.4 %	Sigma-Aldrich, Munich (GER)	T8154
Trypsin-EDTA stock solution (10x)	Invitrogen, Darmstadt (GER)	15400-054
Tryptic soy broth	Sigma-Aldrich, Munich (GER)	22092-500G
Tween-20	Sigma-Aldrich, Munich (GER)	P7949-500ML
Weigert's haematoxylin, stock solution A	Morphisto, Frankfurt (GER)	10225A.02500
Weigert's haematoxylin, stock solution B	Morphisto, Frankfurt (GER)	10225B.02500
Xylene	Sigma-Aldrich, Munich (GER)	16446

Table 2: Cell culture media and solutions

Media/Solution	**Composition**	
0,05% Trypsin/EDTA	10%	0,5% Trypsin-EDTA solution in PBS^-/EDTA solution
Ascorbic acid 2-phosphate solution	73 mg/mL	Ascorbic acid 2-phosphate in E1 media, sterilized before use
300mM Calcium chloride solution	44 mg/mL	Calcium chloride dihydrate in ultrapure water, sterilized before use
Dispase solution	2 U/mL	Dispase in PBS^-, sterilized before use
E1 media	1% 1%	Penicillin/Streptomycin HKGS in EpiLife
E2 media	0,48%	Calcium chloride solution in E1 media
E3 media	0,1% 0,1%	Ascorbic acid 2-phosphate solution KGF solution in E2 media
KGF solution	10 µg/mL	KGF in EpiLife

Mowiol-DAPI mounting solution	0,1%	DAPI in Mowiol 4-88
MTT solution	1 mg/mL	MTT in PBS^-
PBS^-/EDTA solution	0,2 mg/mL	EDTA in PBS^-
Tryptic soy (TS) agar	30 g/L 15 g/L	Tryptic soy broth powder Agarose in DI water, sterilized before use

Table 3: Chemicals and solutions used for histology

Solution	**Composition**	
0,1 % Triton solution	0,10%	Triton in PBS^-
Blocking solution	5%	Donkey serum in antibody dilution solution
Citrate buffer 10x	42 mg/mL 17,6 mg/mL	citric acid monohydrate sodium bicarbonate in DI water
PBS solution 0,5 M (PBS^-)	9,55 mg/mL	PBS^- powder without calcium and magnesium in DI water
Tris/EDTA buffer	1,2 mg/mL 1,5 mg/mL	Tris EDTA in DI water
Washing buffer PBS^- Tween	10% 0,5%	PBS solution 0,5 M Tween-20 in DI water

Table 4: Antibodies

Antigen target	**Isotype Antibody species**	**Dilution**	**Producer**	**Catalog No**
Filaggrin	IgG Rabbit	1:1000	Abcam, Cambridge (UK)	ab81468
Involucrin	IgG1 Mouse	1:100	Thermo Fisher Scientific, Dreieich (GER)	MA5-11803
Stearyl-CoA desaturase-1	IgG Rabbit	1:100	Abcam, Cambridge (UK)	ab39969
Ceramide species	IgM Mouse	1:100	Sigma-Aldrich, Munich (GER)	C8104
Anti-rabbit secondary antibody	IgG Donkey	1:400	Invitrogen, Darmstadt (GER)	A31571
Anti-mouse secondary antibody	IgG Donkey	1:400	Invitrogen, Darmstadt (GER)	A31573

2.2 Equipment

Table 5: List of equipment

Equipment	Device Producer
Accu-jet® pro pipettor	Brand, Wertheim (GER)
Analytical balance	Kern, Balingen-Frommern (GER)
Aspiration Device: VacuBoy	Integra Biosciences, Fernwald (GER)
Autoclaves: Tecnoclav Table-top Autoclave Varioclave	 Biomedis, Gießen (GER) Systec, Wettenberg (GER) H+P, Hackermoos (GER)
Blocking station EG1150H	Leica, Wetzlar (GER)
Cassette printer VCP 5001	Vogel Medizintechnik, Gießen (GER)
Cold storage room, 4 °C	Genheimer, Hochberg (GER)
Cell incubator Haraeus BBD 6220, 37 °C, 5 % CO2	Thermo Fisher Scientific, Dreieich (GER)
Centrifuges: Sorvall Legend X1R Centrifuge 5417R Micro Centrifuge	 Thermo Scientific, Dreieich (GER) Eppendorf, Hamburg (GER) Carl Roth, Karlsruhe (GER)
Cooling plate EG 1150C	Leica, Wetzlar (GER)
Digital camera	Canon, Krefeld (GER)
Drying ofen	Memmert, Schwabach (GER)
Embedding center Microm STP120	Thermo Fisher Scientific, Dreieich (GER)
Freezer -20 °C	Liebherr, Biberach a. d. Riss (GER)
Freezer -80 °C	Thermo Scientific, Waltham (USA)
Freezing container: Mr. Frosty	VWR, Darmstadt (GER)
Hot Air Sterilizer	Memmert, Schwabach (GER)
Ice machine AF-80	Scotsman, Milan (I)
Incubator shaker	Infors, Basel (CH)
Laboratory dish washer	Miele, Gütersloh (GER)
Laminar air flow cabinet Safe 2020	Thermo Fisher Scientific, Dreieich (GER)
LCR HiTESTER 3522–50	Hioki, Japan
Liquid nitrogen storage tank MVE 815 P190 (-180 °C)	German-cryo, Ju chen (GER)
Microplate reader Tecan Infinite M200	Tecan, Crailsheim (GER)
Multistep pipette Multipette M4	Eppendorf, Hamburg (GER)
Microscopes: Biorevo BZ-9000 Evos® AMG	 Keyence, Neu-Isenburg (GER) Life technologies, Darmstadt (GER)
Neubauer cell counting chamber	Hartenstein, Wu rzburg (GER)
Orbital shaker	neoLab, Heidelberg (GER)
Paraffinized Tissue Floating Bath: Type 1052	Medax, Kiel (GER)
Pipettes: 0,5–10 µl, 10–100 µl, 100–1000 µl	Eppendorf, Hamburg (GER)
Platform shaker	neoLab, Heidelberg (GER)
Raman spectrometer	Celltool, Bernried (GER)

Septophag	Hesse, Emmerich (GER)
Slide printer VSP 5001	Vogel Medizintechnik, Gießen (GER)
Sliding microtome SM 2010R	Leica, Wetzlar (GER)
Steamer “Multi Gourmet”	Braun, Kronberg (GER)
Vortex Genie 2	Scientific Industries, Inc., New York (USA)
Water bath	Memmert, Schwabach (GER)
Water purification system	Millipore, Schwalbach (GER)

3. Methods

3.1 Cell culture

3.1.1 Isolation of primary keratinocytes

Keratinocytes were isolated from human juvenile foreskins, donated with informed consent and ethical approval granted by the ethical committee of the University of Würzburg (182/10). Tissue media was sampled to check for microbial contamination. The foreskin was washed twice with Dulbecco’s phosphate-buffered saline (PBS^-) before removal of adipose tissue. The tissue was cut into small stripes, approximately 1-2 millimeters in width, and incubated with 10 mL dispase (2U/mL) at 4 °C overnight. On the following day the epidermis was separated from the dermis and washed again with PBS. Afterwards the epidermal pieces were incubated in prewarmed 10 mL trypsin/EDTA solution (0.5%), for 5 minutes in the water bath at 37 °C. The falcon tube was kept in motion by swirling and vortexing to optimize enzyme activity. After 5 minutes the trypsin enzyme reaction was stopped by adding 1 mL fetal calf serum (FCS). To liberate the cells out of the tissue further mechanical force was applied through up-and-down pipetting and subsequent cell straining. The cells were spun down in a centrifuge (300 x g; 5 minutes; 20 °C) and resuspended in cell media, EpiLife® (Life Technologies) supplemented with human keratinocyte growth supplement (Life Technologies) and Penicillin/Streptomycin from now on referred to as “E1”. After an approximating count using a Neubauer Chamber®, T175 cell culture flasks were seeded with approximately $1.14*10^4$ cells/cm^2 keratinocytes

and grown in the incubator at 37 °C in a humidified atmosphere containing 5% CO_2. All incubation steps below will refer to these conditions.

3.1.2 Passage and subcultivation

The keratinocytes were passaged when they reached 80-90% confluence. After visually checking the medium was aspirated and cells were washed with PBS. Cells were detached by adding 0.04 mL/cm^2 StemPro Accutase® and incubated for 20 minutes. Successful detachment was confirmed with microscopy and the cell suspension was centrifuged (300g; 5 minutes; 20 °C). For cell counting, the supernatant was discarded and the cell pellet was resuspended in E1 media. Cell culture flasks were seeded with approximately 3*10^3 cells/cm^2.

3.1.3 Cryopreservation and thawing

For the cryopreservation the cells were detached from cell culture flasks as described above (see 3.1.2.). Cryovials were filled with 1 mL of cell suspension with approximately 3*10^6 cells per mL E3 media and frozen after adding 10% DMSO. The cells were frozen using a MrFrosty™ Freezing Container at -80 °C and were transferred to the liquid nitrogen storage at -176 °C after 24 hours. When needed, the cryovials were thawed using 9 mL of prewarmed E3 media by pipetting 1 mL at a time to directly extract cells from the frozen media and returning them immediately into warm media.

3.1.4 RHE model construction

For the generation of RHE models keratinocytes from the 2nd passage were used. The morphology and the confluence of keratinocytes was checked under the microscope (See Figure 1). The method of detachment was described earlier (section 3.1.2) except the media used for resuspension was E1 supplemented with 1.5mM $CaCl_2$ (referred to as E2). After cell counting the cell suspension was diluted to 6*10^5 cells per mL and 500 µL were seeded onto Millicell® cell culture insert (pore size 0.4 µm; cell culture area 0.6 cm^2 which were placed in a 6-well cell culture plate. The cells were allowed to adhere to the insert membrane for 2

hours in the incubator before 2.5 mL E2 media was added to the well below the insert. After 24 hours the E2 media was removed from both the inside and the outside of the insert and replaced with 1.5 mL of E3 media per well except only outside of the insert. This established an ALI. The E3 media is based on the E2 media, which is additionally supplemented with 73 µg/mL L-ascorbic acid 2-phosphate and 10 ng/mL keratinocyte growth factor. The ALI phase lasts 19 days until the RHE models are used for testing. This procedure will be referred in this study as “standard protocol”.

3.1.5 Modifications to the standard protocol

Lipid supplementation

For the supplementation of lipids the standard protocol was modified. Lipid mixture 1 by Sigma Aldrich (referred to as “LipidMix”), a chemically defined solution of lipids, was added additionally to the E3 media (see table 6). A range of concentrations recommended by the manufacturer from 1 mL up to 10 mL per liter E3 media was tested. The supplemented E3 media was added on day 1 of the ALI phase. The duration of the culture phase did not change and was kept for 19 days.

Table 6: Lipid mixture 1 lipid components

Substrate	Concentration
Arachidonic acid	2 µg/ml
Linoleic acid	10 µg/ml
Linolenic acid	10 µg/ml
Oleic acid	10 µg/ml
Palmitic acid	10 µg/ml
Myristic acid	10 µg/ml
Stearic acid	10 µg/ml
Cholesterol	0.22 mg/ml

Glycolic acid treatment

RHE models were cultured according to the standard protocol up to day 17 of the ALI culture phase. On day 17 glycolic acid (GA) was applied on top of the SC in various concentrations and put back into the incubator for different amounts of time. The variables chosen were application durations of 5, 15 and 30 minutes

and GA concentrations of 1%, 2%, 5% and 10%. After incubation the RHE models were washed thrice with PBS^- and residual PBS^- was removed by vacuum aspiration. RHE modes were cultured for two more days before harvest and testing.

3.2 Methods used for characterization and evaluation of RHE models

3.2.1 Barrier test

After 20 days of culture in total, on day 19 of the ALI culture phase, the RHE modes were ready for testing. 50 µL triton X-100 (1% w/v) was topically applied on the SC and returned to the incubator. After 2 hours the RHE modes were washed 6 times with 800 µL PBS^+ and residual PBS^- was removed by vacuum aspiration. The RHE modes were moved to a new 24-well plate with 200 µL MTT solution (1mg/mL). After ensuring the absence of air bubbles underneath the polycarbonate membrane - the RHE models were returned to the incubator for another 3 hours. Then the inserts were removed from the MTT-containing wells and blotted on an adsorbent paper in order to remove droplets of MTT solution adhering to the outer insert wall and the outer membrane. RHE models were transferred in a new 24-well plate and submerged in 2 mL isopropanol to extract formazan. This process was done overnight (approximately 16-18 hours) at 4 °C. . Homogeneity of the solution was ensured by piercing the insert membrane with a cannula and pipetting up and down. The optical density (OD) of the formazan solution was measured in a spectrophotometer at a wavelength of 570 nm, using isopropanol as blank.

3.2.2 ET50 test

RHE model triplets were subjected to Triton X-100 (1% w/v) treatment for 1.5, 3, 4.5 and 6 hours in the incubator. An untreated triplet served as a control group. After treatment the RHE models were washed 6 times with 800 µL PBS^+ and residual PBS^- was removed by vacuum aspiration. Following procedures mirror the barrier test as described above (see 3.2.1.).

3.3 Histological characterization of RHE

3.3.1 Fixation of tissue samples

For histological analysis the RHE models were fixed in 4% paraformaldehyde for 2 hours. Then the RHE model and the polycarbonate membrane were cut out from the insert using a scalpel blade and transferred to an embedding cassette. The embedding cassette was left for another 2 hours in deionized (DI) water to wash out remaining paraformaldehyde. Table 7 describes subsequent steps done to embed the samples into paraffin.

Table 7: Steps of paraffin embedding

Duration [h]	Solution	Step
1	DI water	Washing
1	Ethanol 50%	Dehydration
1	Ethanol 70%	
11	Ethanol 80%	
1	Ethanol 96%	
1	Isopropanol I	
1	Isopropanol II	
1	1:2 Isopropanol-Xylol mixture	Alcohol removal
1	Xylol I	
1	Xylol II	
1.5	Paraffin I	Paraffin embedding
1.5	Paraffin II	

Once embedded in paraffin the RHE model is intersected in the middle to acquire 2 half circles of tissue. These are casted into a paraffin block using a metal mould. After cooling the solid paraffin block was removed from the metal mould and 3.5 µm cuts were made using a microtome. The paraffin cuts were transferred onto a polylysine slide and residual water was dried off in a heat chamber at 37 °C. Afterwards the slides were transferred into a 60 °C heat chamber to melt off the paraffin. The following steps to completely remove the paraffin and rehydrate the tissue sample are listed in table 8.

Table 8: Steps of rehydration

Duration [min]	Solution	Step
10	Xylol I	Paraffin removal
10	Xylol II	
Submerge thrice	Ethanol 96% I	Rehydration
Submerge thrice	Ethanol 96% II	
Submerge thrice	Ethanol 70%	
Submerge thrice	Ethanol 50%	
Swivel until no more turbulences can be observed	DI water	Alcohol removal

3.3.2 Haematoxylin-Eosin stain

The haematoxylin-eosin (H&E) stain aims to provide an overview of cell and tissue morphology. Haematoxylin stains basophilic structures like deoxyribonucleic acid (DNA) and highlights the cell nuclei of tissue cells. Meanwhile eosin colors acidophilic tissue such as structural proteins, thus the cytoplasm, red. After paraffin removal the slides are submerged in haematoxlin staining solution for 6 minutes. Any residual staining solution was washed off using DI water and the slides were transferred into tap water to trigger the blue color of the haematoxylin dye through a higher pH. The slides were then counterstained using an eosin solution for another 6 minutes. The washing step with DI water was repeated to remove left over dye and dehydration was performed according to the procedure listed in table 9. The slides were covered in permanent mounting media Entellan and a cover slide.

Table 9: H&E staining followed by dehydration

Duration [min]	Solution	Step
8	Haemalaun	Stain basophilic structures
-	DI water	Rinse until solution is clear
5	Tap water	Blueing
1	Eosin	Stain acidophilic structures
-	DI water	Rinse until solution is clear
Submerge twice	Ethanol 70%	Dehydration
2	Ethanol 96%	
5	Isopropanol I	
5	Isopropanol II	
5	Xylol I	Alcohol removal
5	Xylol II	

3.3.3 Immunofluorescence

This method aims to visualize macromolecules through specific antigen-antibody binding and secondary antibodies coupled with fluorescent dye, which can be analyzed under a fluorescence microscope. After sample preparation and rehydration, the epitopes of the tissue were unmasked using heat. Sample slides were submerged in citrate buffer (pH 6.0) within a metal bowl and cooked in a steamer for 20 minutes. After unmasking the slides were transferred back into DI water. The area of the sample was encircled using a grease pen to improve efficiency of the antibody solutions. A 5% blocking solution consisting of antigen of the same species as the secondary antibody was applied for 20 minutes in a humidity chamber to minimize unspecific interaction. The blocking solution was removed by shaking it off. Table 11 lists the dilution of the primary antibody which were applied and incubated overnight at 4 °C within the humidity chamber. The amount of antibody dilution was dependent on sample size.

Table 10: Antibody details

Antigen target	**Antibody species**	**Dilution**	**Isotype**	**Description**
Filaggrin	Rabbit	1:1000	IgG	Primary AB
Involucrin	Mouse	1:100	IgG1	Primary AB
Stearyl-CoA desaturase-1	Rabbit	1:100	IgG	Primary AB
Ceramide species	Mouse	1:100	IgM	Primary AB
Rabbit antibody	Donkey	1:400	-	Secondary AB
Mouse antibody	Donkey	1:400	-	Secondary AB

After incubation the slides were washed thrice for 5 minutes on a shaker using PBS-tween washing buffer. The secondary antibody dilution was applied and the samples were incubated for 60 minutes in the dark humidity chamber at room temperature. Once more the remaining antibody solution was discarded and the slides were washed thrice for 5 minutes on a shaker using PBS-tween washing buffer. Finally the slides were covered with a mounting solution containing Moviol and 4' 6-diamidino-2-phenylindole (DAPI) which binds to DNA and indicates the cell nuclei. To eliminate false positives through unspecific binding following controls were done. Isotype controls were made by replacing the primary antibody using an antigen containing the same constant region of the primary antibody. The control for the secondary antibody was done without using any

primary antibody at all. Signal strength of the region of interest was quantified by using ImageJ [42].

3.4 Raman spectroscopy

3.4.1 Sample preparation

Epidermal models were harvested on day 19 of the ALI culture. The model was cut out of the insert using a scalpel and a cross-section was embedded in TissueTek® O.C.T. Compound (Sakura). The cryotome sample blocks were left initially at -20 °C to solidify and later moved to -80 °C for prolonged storage. Two cryotome sections with a thickness of 10 µm were made for each sample slide. The RHE model sections were then immersed in DI water for 5-10 minutes to dissipate the embedding compound. Afterwards sections were covered with DI water to prevent the samples from drying out.

3.4.2 Raman spectra measurement

For the collection of Raman spectra the BioRam (CellTool GmbH) system with a non-destructive 785 nm laser was used. This system combines Raman spectrometry with digital microscopy and was calibrated using a standard silicon sample. All molecules within the laser focus contribute to a sum spectrum resulting in a unique fingerprint. First the sample slides were focused on the layer of interest using the water immersion objective. For each sample 6 different measure coordinates were chosen within the SC layer. The Raman spectra were taken using accumulated scans of 3 times 10 seconds and an excitation power of 80 mW.

3.4.3 Raman data pre-treatment and multivariate data analysis

Raman spectroscopic data were processed applying customized software by CellTool GmbH. Data were cropped to 500–1700 cm^{-1} representing a wavenumber range with high amount of biological information [43]. Then, a baseline correction with asymmetric least squares smoothing was applied.

Further data pre-treatment with a median filter for data smoothing and subsequent multivariate data analysis were done with the statistical software “The Unscrambler X 10.4” (Camo Software, Norway). Finally mean spectra were calculated and displayed in “The Unscrambler X 10.4”.

3.5 Impedance spectroscopy

The measurement were done on the final day of the ALI culture shortly before the application of the irritant Triton X-100 (1% w/v) for either MTT test or the ET50 test as detailed in chapter 3.2.1 and 3.2.2 respectively. The RHE models were transferred into a new 24-well culture plate containing 500 µL E3 media. Another 500 µL E3 media was applied topically on the SC of the RHE models. Electrodes of the LCR HiTESTER 3522–50 (Hioki, Japan) were introduced on both sides of the well insert. During the measurement the spectrum containing 40 data points was taken exponentially from 1 Hz to 100 kHz. Each data point was represented by 4 RHE models each and the average mean impedance (Ohm) was calculated.

3.6 Transepidermal waterloss (TEWL)

Similar to impedance measurements TEWL was also measured on the final day of the ALI culture before irritant application. A custom-made adapter (see Fig 10a) was used to enable TEWL measurements using the Tewameter® TM 300 by Courage Khazaka. Measurements were done in a 6-well culture plate well filled with 1.5 mL E3 media. Each model of the triplet was measured thrice. Additional distance of the adapter method was corrected by using the formula provided by Courage Khazaka.

3.7 Microbiology

Staphylococcus epidermidis ATCC12228 strain which was used in this experiment was acquired from Prof. Dr. Wilma Ziebuhr, Institute for Molecular Infection Biology (IMIB) University of Würzburg.

3.7.1 Storage and preparation

Isolated colonies were obtained by streaking out bacteria on tryptic soy agar plates. The bacteria were incubated at 37 °C for 48 hours and stored at 4 °C for further use. For each colonization experiment, an overnight culture was inoculated on day 18 of the ALI phase of the RHE model.

3.7.2 Colonization of RHE models with S. epidermidis

To minimize the effects of antibiotics added to E3 media, the antibiotics were removed on day 16 of the ALI phase during media change to allow any residual antibiotics to be washed out until bacterial colonization on day 19. An overnight culture (ONC) was prepared in 5 mL TS broth on day 18. The optical density at 600 nm (OD_{600}) of the ONC was determined using a multiplate spectrophotometer (JASCO V-730). The ONC was serially diluted by a factor of 1:10 until a 10^6 dilution was reached. 100 µL of the 10^4, 10^5 and 10^6 dilutions were plated on agar plates as these dilutions have resulted in countable numbers of colony forming units (cfu) in previous experiments. The yielded cfu numbers were used to calculate theoretical numbers of S. epidermidis applied on the models. For colonization, 100 µL of 10^2 to 10^6 dilutions were topically applied to cover the whole surface of the model. The media underneath the models were refreshed with E3 media without Penicillin/Streptomycin and the models were returned to the cell culture incubator for 48 hours.

3.7.3 Sample preparation and fixation for scanning electron microscopy

As previously described antibiotics were removed from cell culture media 2 days prior to bacterial application. The cell growth of S. epidermidis ONC was measured using photometry and a 1:10 dilution was made which approximated to $1{,}9*10^7$ cfu/mL. In a few washing steps tryptic soy broth media was replaced with PBS^-. First the bacteria suspension was spun down using a centrifuge (16000 g, 5 minutes, 4 °C). Then the supernatant was removed by vacuum and the pellet was resuspended in PBS^-. These steps were repeated twice. 100 µL of the bacterial suspension were applied topically on each RHE model and returned to the incubator for 24 hours. The RHE models were washed thrice using 800 µL

PBS^-. RHE models were cut out of the insert and fixated using 6% glutaraldehyde on ice for 15 minutes. Table 9 describes the following steps for dehydration. RHE models were stored in 100% acetone for critical point drying.

Table 9: Critical point aceton dehydration

Duration [min]	Solution	Step
5	PBS^-	Washing step repeated 5 times, on ice
15	30% Acetone	Dehydration, at room temperature to avoid condensation moisture
20	50% Acetone	
30	75% Acetone	
45	90% Acetone	
30	100% Acetone	Repeated 6 times

After critical point drying the samples were sputtered with gold-palladium and examined under a scanning electron microscope (SEM).

3.8 Statistical analysis of data

All data points obtained from experiments were used as inputs in GraphPad PRISM 6. Statistical analysis of data triplets was done using one-way analysis of variance (ANOVA) and a Dunnett's multiple comparison test.

4. Results

The aim of this thesis was to improve barrier capability of in-vitro RHE models, in comparison to the current protocol, to eventually achieve a representative value approximate to native human skin. In order to achieve this, different approaches such as topical GA application and LipidMix supplementation were evaluated during an initial round of testing involving the less resource-intensive barrier test and standard H&E staining histology tests. Based on these results, the most promising approach was further explored and analyzed. The ET50 test was used to confirm and expand quantitative results obtained from initial barrier tests. Histological and immunohistochemical (IHC) stainings were used to show morphological changes and highlight structural protein expression within the RHE models. Impedance was measured as a correlative property of the barrier function using impedance spectroscopy. Furthermore, TEWL was measured and Raman spectroscopy was used to detect qualitative changes concerning the lamellar lipids packing state. Thesecharacterization methods serve to give a better understanding on how the protocol modifications influence the barrier function.

4.1 Effects of topical glycolic acid application

In this experiment, RHE models were treated with GA 2 days prior to the barrier test. This test demonstrates the barrier function of the SC when an irritant such as Triton X-100 (1% w/v) is topically applied. Depending on the strength of the barrier the vulnerable cells underneath the SC are damaged, which causes a reduced metabolic activity. The reduced metabolic activity is shown by a MTT test. In this approach, parameters included various concentrations of GA ranging from 1% to 10% and varied in application duration from 5 minutes up to 30 minutes. The results show similar values for lower concentrations and short incubation times (see Fig. 3). Treatment using 1% GA resulted in reduction of viability by 8.6% and 7.6% for 5 minutes and 15 minutes respectively. 5 and 30 minute treatments with 2% GA maintained RHE viability at a close level to the control, while the 15 minute treatment reduced viability by 7.1%. While 5 minutes of 5% GA only showed a reduction by 3%, further treatment time decreased RHE

viability after 15 and 30 minutes by 79.4% and 87.4%. A treatment of 10% GA for 30 minutes resulted in a viability reduction by 99.3%.

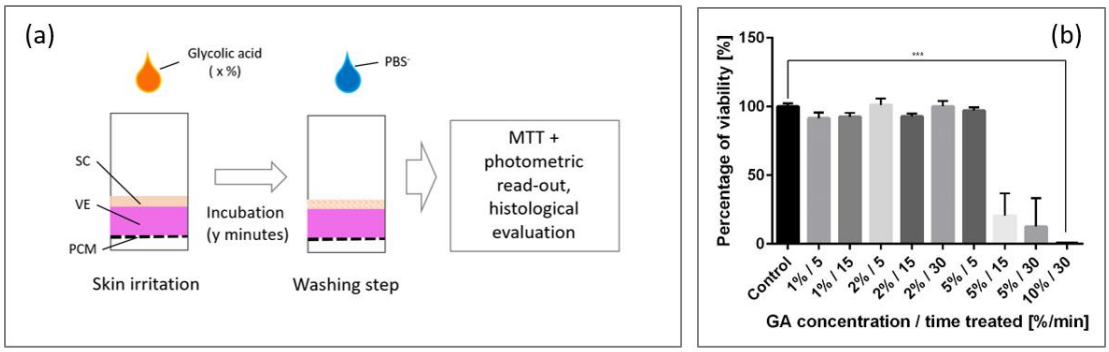

Figure 3: ***Scheme (a) and results (b) of glycolic acid (GA) application****: The percentage of viability of skin models after being treated with GA. All skin models were cultured with the current open-sourced protocol. GA was applied with different time spans and concentrations on the 18th day of culture Resulting values were normalized to the control group. SC = stratum corneum; VE = Viable epidermis; PCM = Polycarbonate membrane; PBS = Phosphate buffered saline; (Mean ± SD; **P<0.01, ***P<0.001 control, n=3 independent experiments; one-way ANOVA)*

The morphological structure of a tissue is an important reference, since it also serves as a control for the proper model growth. To compare modifications to the established standard protocol of RHE models, histological haematoxylin-eosin and immunohistochemical staining methods were used. Sections of RHE models and native skin were stained to highlight typical morphologies of the different human skin layers. The haematoxylin-eosin staining allowed differentiation between the protein-rich SC and living cells of the epidermis made up of layers SB, SS and SG. All RHE models formed a multilayered tissue over a culture period of 19 days (see Fig. 4). The SC, the uppermost layer, is thicker in RHE models compared to the native skin sections. HEK in the SG layer differ compared to native skin by being mostly flat, but still display the eponymous small granules. Also some cells have lost their nuclei. While the RHE models show a constant thickness of the SS, it varies greatly due to the presence of dermal papilaries in native skin. Lastly, the SB is formed through a monolayer of uniform cuboid HEK in both RHE models and native skin sections. No significant changes were observed between RHE models of different protocols.

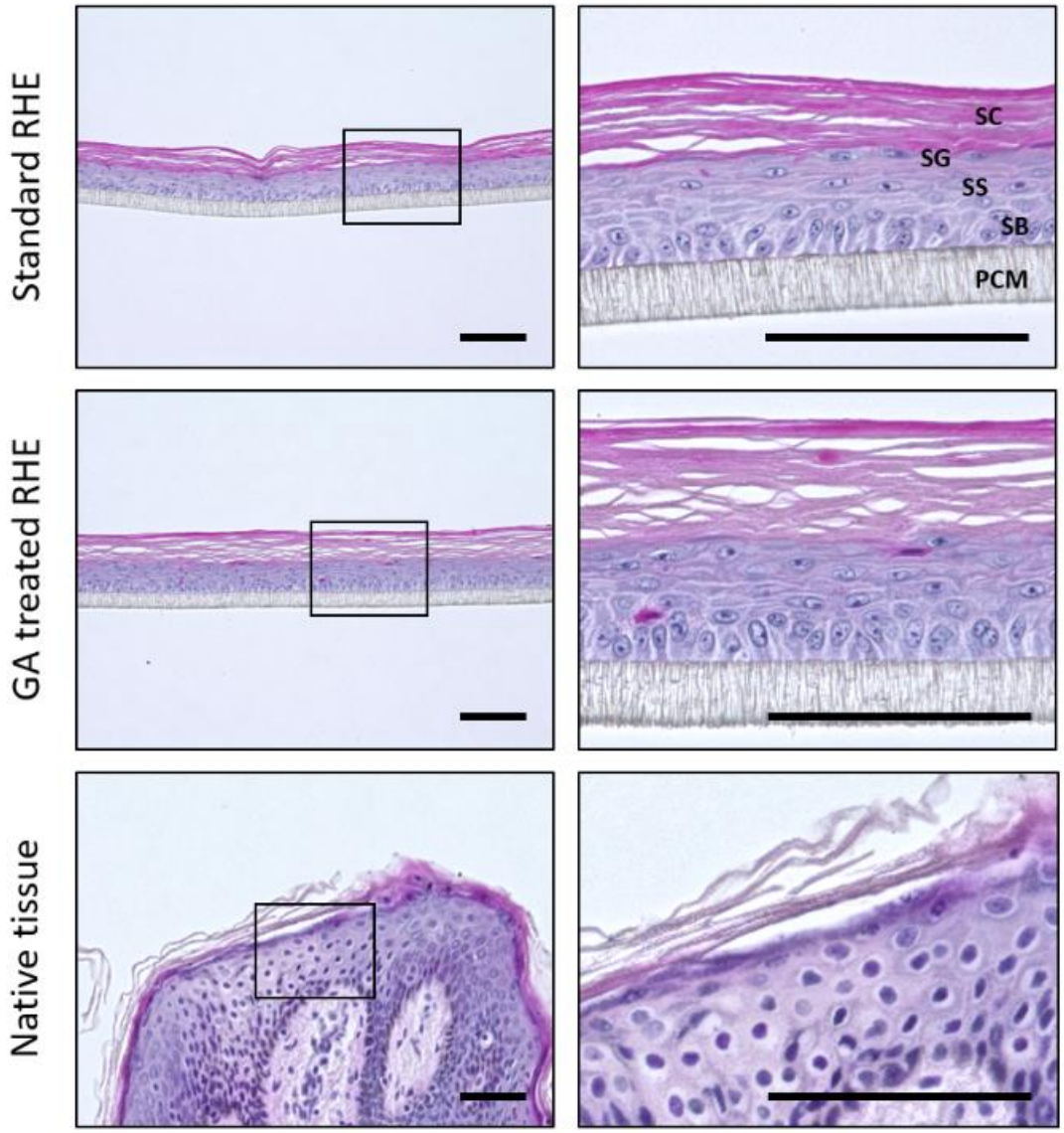

Figure 4: ***Brightfield microscopy pictures****: Histological evaluation of haematoxylin-eosin stained cross-sections obtained from different RHE models and native human foreskin. RHE models were cultured either according to current standard protocol or treated with 2% concentrated glycolic acid for 5 minutes on day 17 during the standard. SC = stratum corneum; SG = stratum granulosum; SS = Stratum spinosum; SB = stratum basale; PCM = polycarbonate membrane; Scale bar represents 50 µm*

4.2 Effects of LipidMix supplementation and further characterization

4.2.1 Barrier test and histological assessment

For the experiments focusing on lipid supplementation, an optimal concentration was found by testing various concentrations of LipidMix (see Fig. 5a). The range of concentrations, 1 mL/L to 10 mL/L, was recommended according to the manufacturer specification. Further experiments involving lipid supplementation were done using a concentration of 1 mL/L LipidMix, which showed the best effect increasing viability by 19%. Figure 5b and Figure 5c show the effect of LipidMix supplementation in three independent iterations of the experiment. Each experiment was done using a triplet of RHE models as sample size. The positive effect on barrier capability can be seen on both RHE models, derived from two different donors in varying effect magnitude. The RHE models, derived from donor 13-037, showed an increase of 12%, 16% and 19%, while RHE models, cultured using keratinocytes from donor 15-012, showed an increase of 8%, 18% and 13% respectively. The histological assessment showed a slight penetration of eosin-stained material through the SG (see Fig. 6). However, as mentioned above, no further significant changes were observed using the H&E staining method.

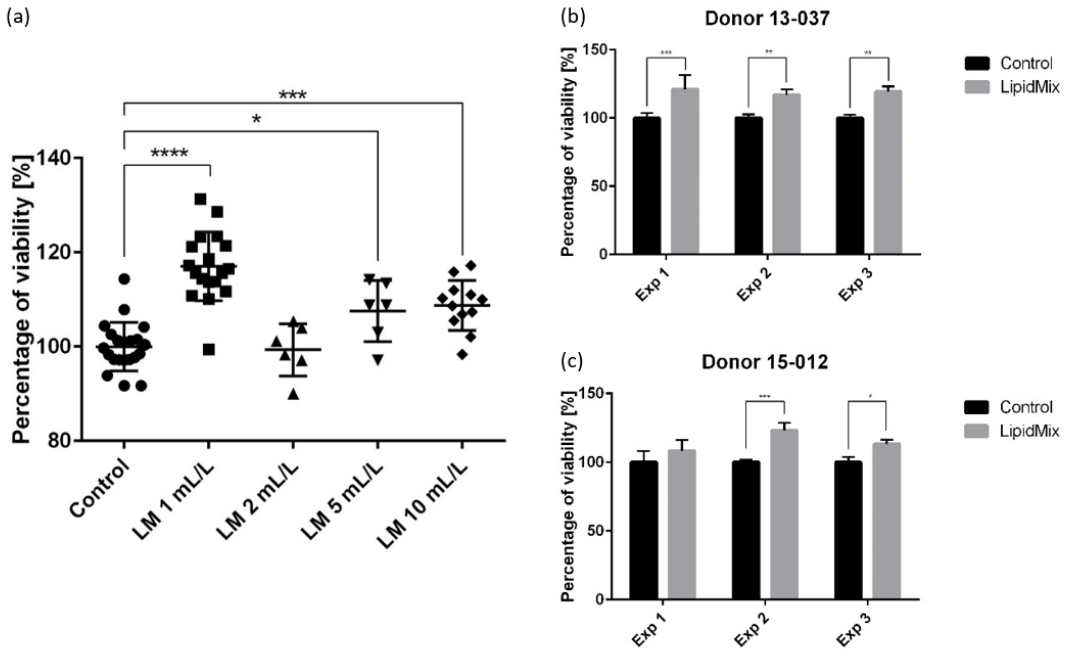

Figure 5: ***MTT barrier test results;*** *(a) Comparison between the effects of modified protocols using different concentration of the supplement „LM" (LipidMix). n(Control) = 21; n(LM 1 mL/L) = 18; n(LM 2 mL/L) = 6; n(LM 5 mL/L) = 6; n(LM 10 mL/L) = 12. The models from Donor 13-037 (b) and 15-012 (c) and their percentage of viability after treating the models for 2 hours with Triton X-100 (1% w/v). Skin models with added supplements (1 mL/L LipidMix) were labelled as „LipidMix" opposing the current standard protocol as control group. Resulting values were normalized to the control group. The iteration of the experiment has been labelled on the x-axis as Exp 1, 2 or 3 respectively. (Mean ± SD; *P<0.05, **P<0.01, ***P<0.001 control, n=3 independent experiments; one-way ANOVA)*

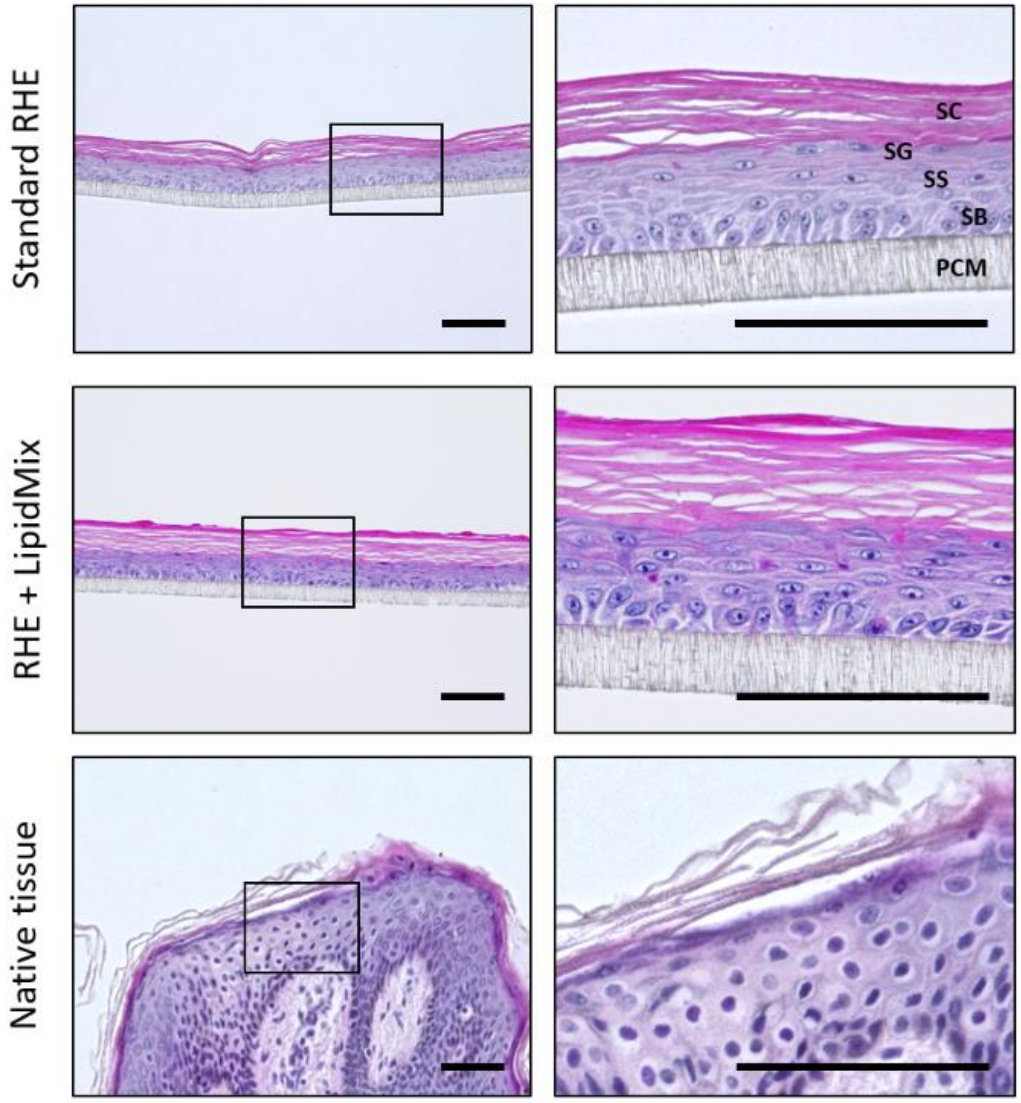

Figure 6: ***Brightfield microscopy pictures****: Histological evaluation of haematoxylin and eosine stained cross-sections obtained from different RHE models and native human foreskin. RHE models were cultured either according to current standard protocol or supplemented with LipidMix. SC = stratum corneum; SG = stratum granulosum; SS = Stratum spinosum; SB = stratum basale; PCM = polycarbonate membrane; Scale bar represents 50 µm*

To further investigate effects of LipidMix supplementation, sections of human foreskin, standard protocol RHE and LipidMix supplemented RHE were stained with immunofluorescence antibodies (see Fig. 7a). To enable quantitative comparison, sections of standard protocol RHE and LipidMix supplemented RHE were stained on a mutual slide and exposure time was kept constant during image capture. Relative fluorescence was digitally quantified using ImageJ (see Fig. 7b). Four antibodies against known markers proteins, each with vital

contributions to creating and maintaining an optimal skin barrier function, were used [44]–[47]. Filaggrin was observed in native tissue as well as in both RHE models almost exclusively in the SC. Fluorescence was increased in LipidMix supplemented RHE models by 99.28% compared to standard protocol RHE. In the native tissue involucrin was mainly present in the layers of SS and SG. This is also true for the standard protocol RHE. In contrast, LipidMix supplemented RHE show weak fluorescence throughout the SC. Comparing the corrected total involucrin antibody fluorescence in both RHE models indicates a decrease in LipidMix supplemented RHE by 43.48%. Stearyl-CoA desaturase-1 (SCD1) observed predominantly in SS and SC show a slightly weaker presence in standard protocol RHE and barely any signal in LipidMix supplemented RHE. Fluorescence signal was reduced by 45.79%. Lastly, signal from antibodies against ceramide species was observed throughout all layers of the native tissue, particularly in cell nuclei of keratinocytes and within the SC. While fluorescence signal was stronger by 98.21% in the LipidMix supplemented RHE compared to the standard protocol RHE, the signal pattern of RHE models differed by showing strong signal outside the cell nuclei and less signal within the SC.

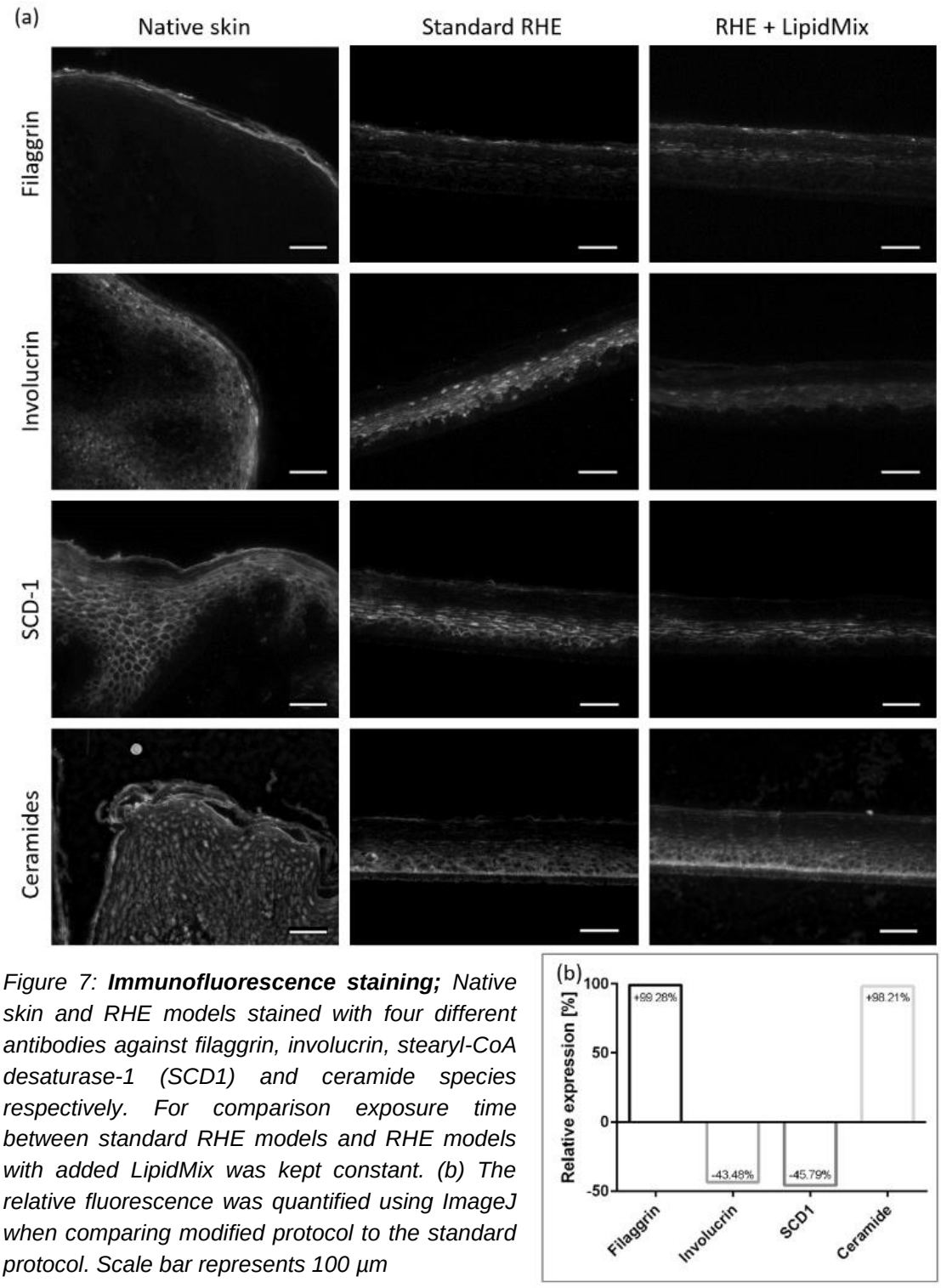

Figure 7: ***Immunofluorescence staining;*** *Native skin and RHE models stained with four different antibodies against filaggrin, involucrin, stearyl-CoA desaturase-1 (SCD1) and ceramide species respectively. For comparison exposure time between standard RHE models and RHE models with added LipidMix was kept constant. (b) The relative fluorescence was quantified using ImageJ when comparing modified protocol to the standard protocol. Scale bar represents 100 µm*

4.2.2 ET50 test

After initial tests using the barrier test, LipidMix supplemented RHE models were further compared to the standard protocol using the ET50 test to reproduce obtained results. While similar to the barrier test described above, this test further

adds an additional dimension by measuring the decrease of viability over time during Triton X-100 treatment. RHE models made using three different donors were tested using this method (see Fig. 8). RHE models derived from donor 13-032 yielded an ET50 value of 2.54 hours when cultured following standard protocol and 2.64 hours when cultured using the LipidMix protocol, resulting an increment of 4%. RHE models derived from donor 14-020 increased from 4.95 hours to 5.27 hours after modification of the standard protocol, increasing the ET50 value by 6.4%. Lastly RHE models derived from donor 15-012 showed an increase of 10.6% from 1.97 hours to 2.18 hours.

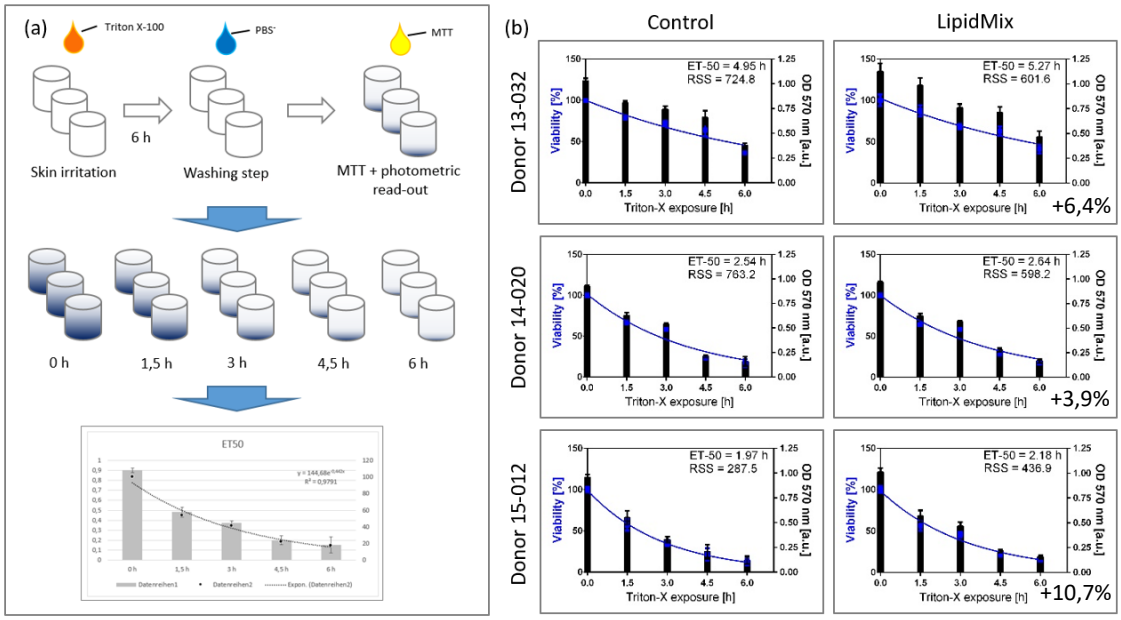

Figure 8: ***Schema (a) and results of ET50 test (b);*** *Test was done using 3 independent donors named 13-032, 14-020 and 15-012. The resulting value called „ET50“ describes the exposure time to an irritant needed to reduce the cell viability within the model to 50%. Skin models with added supplements were labelled as „LipidMix“ opposing the current standard protocol as control group.*

4.2.3 Impedance spectroscopy

Impedance has been correlated to barrier function [48]. Data points acquired from LCR HiTESTER 3522–50 were plotted into a diagram representing frequency and amplitude, after being transformed into the real part of impedance by factoring the phase shift into the amplitude (see Fig. 9b). Transepidermal electrical resistance (TEER) value was calculated by factoring the area of the RHE model surface (0.64 cm²) into the real part of the impedance. Three frequencies, 12.5, 100 and 1000 Hz were chosen to represent relevant data

points for the comparison between different samples (see Fig. 9c). In this experiment, models produced from standard protocol procedure and models supplemented with LipidMix were compared in regards to their electrical resistance, which is another indicator of their barrier function. RHE models cultured using donor 13-032 and 15-012 showed no significant increase in TEER value and donor 14-020 indicated a lowered resistance in models supplemented with LipidMix.

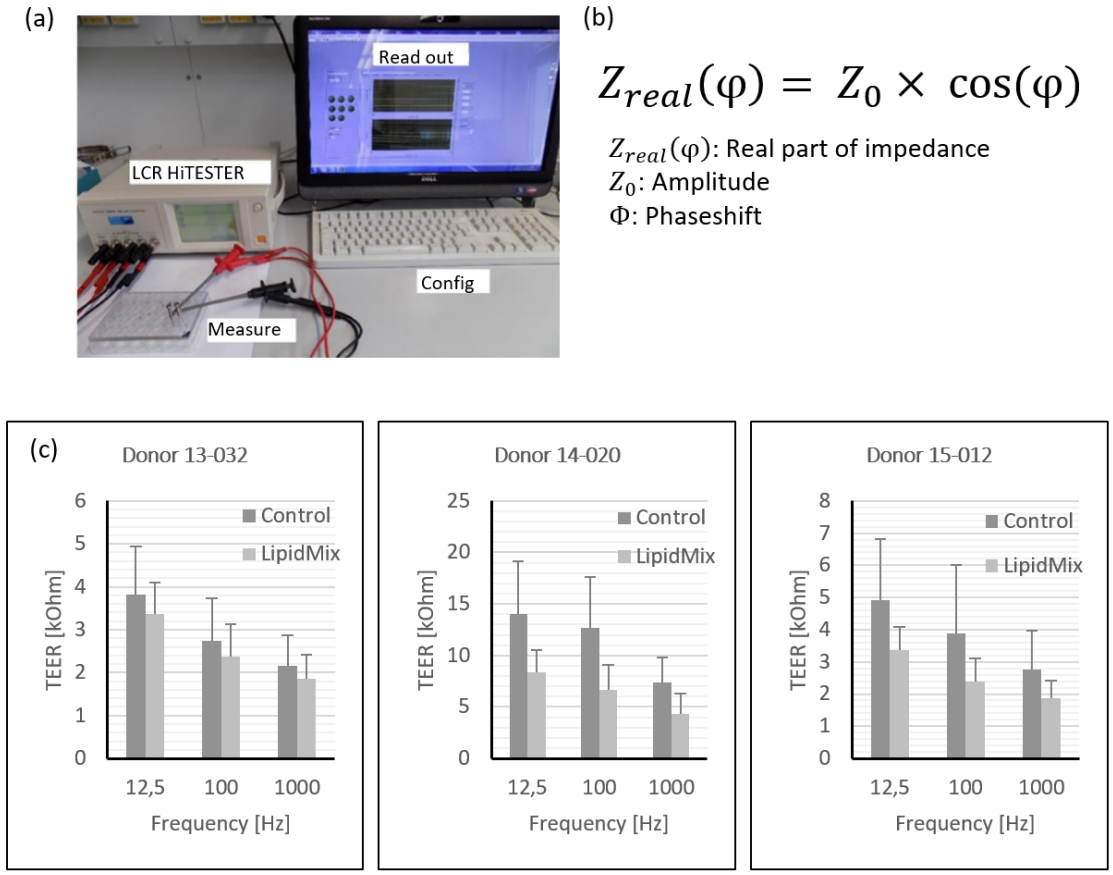

Figure 9: ***Results of impedance measurements;*** *Impedance of standard protocol RHE models and LipidMix supplemented RHE models were measured on day 19 of the air-liquid culture phase. Measurements were done using LCR HiTESTER 3522–50 (Hioki) (a). The real part of the impedance were calculated (b) and transformed into TEER values by factoring in the surface area. Three frequencies were chosen to represent the spectral data (c).*

4.2.4 Raman spectroscopy

Beside the impedance spectroscopy, another non-invasive method was used to gather results, which have been correlated in the literature to the barrier function, Raman spectroscopy [49]. Using Raman spectroscopy, a molecular fingerprint is detected and can be associated with certain biomolecules [43]. This experiment focuses on certain wavelengths corresponding to the ratio of cis/trans-conformed fatty acids within the lamellar lipids of the SC. A ratio in favor of the trans-conformed fatty acids suggests a less dense lateral packing status [50]. This ratio is calculated by dividing the combined relative signal of arbitrary units at wavenumber 1130 and 1030 through the signal measured at wavenumber 1080 (see Fig. 10). RHE models derived from donor 15-012 showed no significant change when standard protocol RHE were compared to LipidMix supplemented RHE. In contrast, RHE models derived from donor 15-017 showed a clear difference in peak patterns. Compared to the standard protocol RHE the signal peaks of the LipidMix supplemented RHE showed a lower value for wavenumber 1130 and 1030 and an increased value for wavenumber 1080. This would suggest a less dense lateral packing status for the lamellar membrane lipids of the SC.

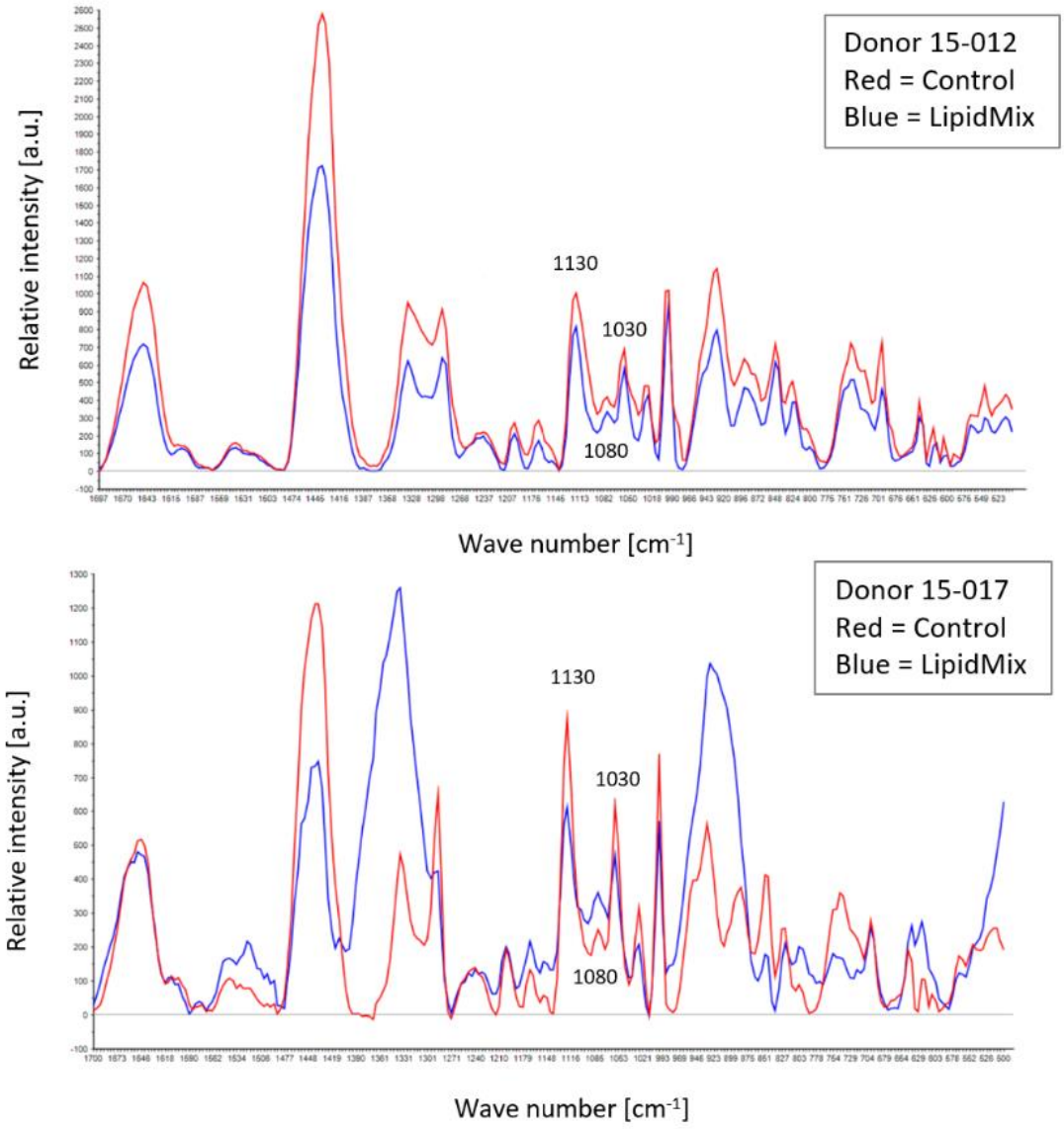

Figure 10: ***Mean Raman specta;*** *In this experiment the focus was the signal ratio of* $S_{(1130+1030)}$:S_{1080}*, which is reported to correspond to packing density of laminar lipids. Data was cropped to biological relevant wave number range. Spectra were normalized and the means displayed in the Unscrambler X 10.4 (Camo). Two independent experiment results involving two different donors are shown in this figure.*

4.2.5 Transepidermal waterloss measurements

Measuring TEWL is one of the traditional techniques dermatologists use to diagnose skin condition and barrier functionality. As such, in this experiment, a Tewameter© TM 300 (Courage Khazaka) was used to measure TEWL values of the RHE models. Usually TEWL is measured by holding the probe directly onto the skin to prevent additional airflow and humidity to distort the result. To enable TEWAmeter measurements for in-vitro RHE models, the method had to be adapted. Therefore, an adapter was designed by 3D computer assisted design (CAD) software SOLIDWORKS and produced to fit the probe on millicell well inserts for measurement (see Fig. 11a). The changed measure distance was compensated using the formular (see Fig. 11e) provided by Courage Khazaka, which is offset by an increased distance of 8 mm between the electrodes and SC. Both standard protocol RHE and LipidMix supplemented RHE models were measured showing an average of 15.8 and 12.47 g/h/m² of TEWL respectively.

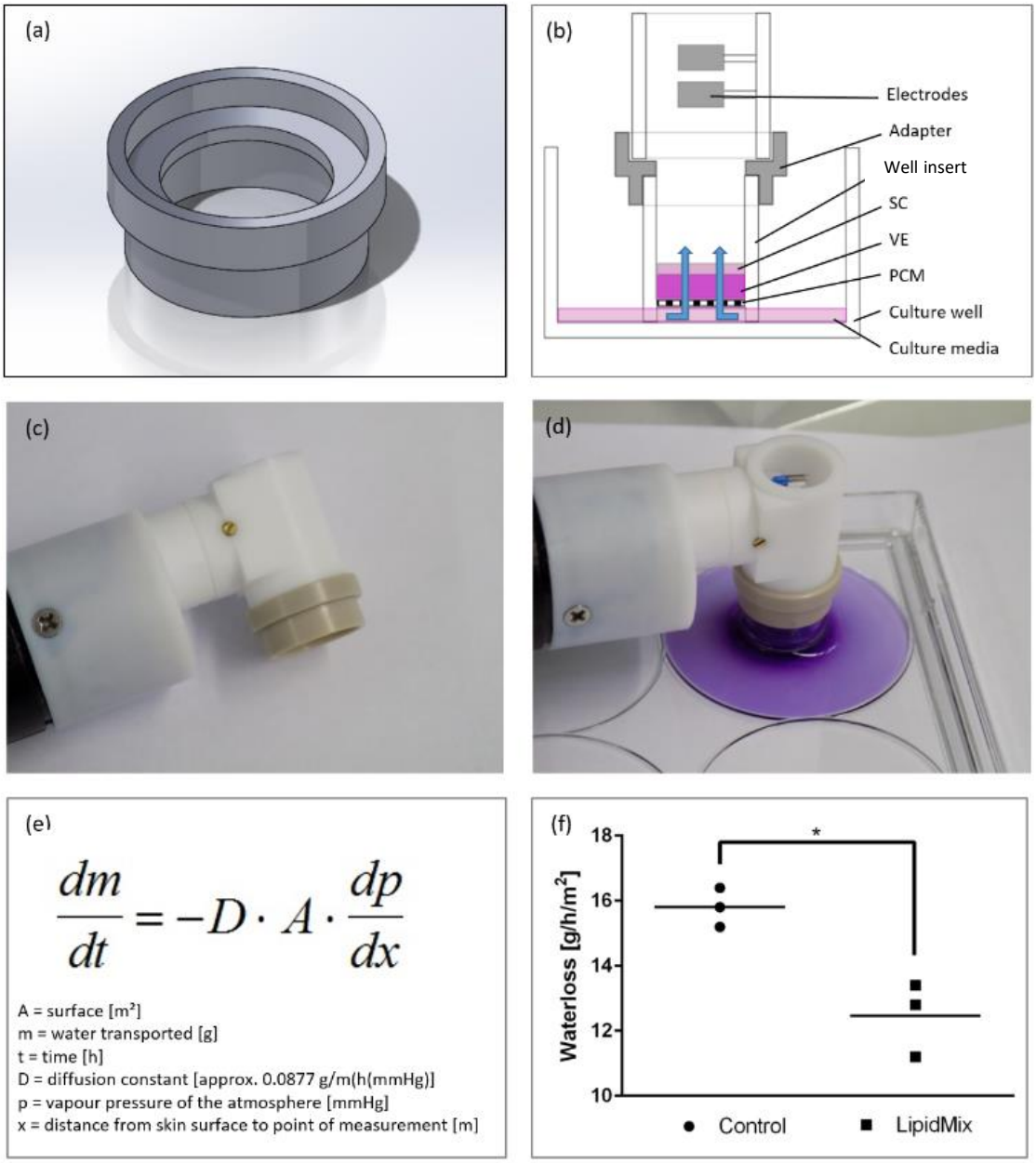

Figure 11: ***Adapter CAD Design (a), scheme (b), Macroscopic images (c,d), formular (e) and results of transepidermal waterloss (TEWL) measurements (f):*** *Measurements were done with Tewameter® TM 300 (Courage Khazaka) using an adapter which was designed with 3D computer assisted design (CAD) construction software SOLIDWORKS. Comparison between control group and 1mL/L LipidMix supplemented RHE skin models. Waterloss is expressed in g/h/m². * P<0.05*

4.3 Adherence of *S. epidermidis* to RHE model surface

Initial attempts revealed difficulties to capture *S. epidermidis* adhering to the RHE model surface. *S. epidermidis* was only observed in models which were not rinsed after vacuuming the residual media (Fig 12a). After changing the incubating media to nutrient-deficient PBS^- bacterial adhesion was induced to the model surface and microbes were observed after the washing steps under reflective-light microscopy (Fig 12b). To obtain further visual confirmation of the bacterial morphology, scanning electron microscopy analysis was performed (Fig 12c). On images with higher resolution, adhesion associated protein strands can be seen.

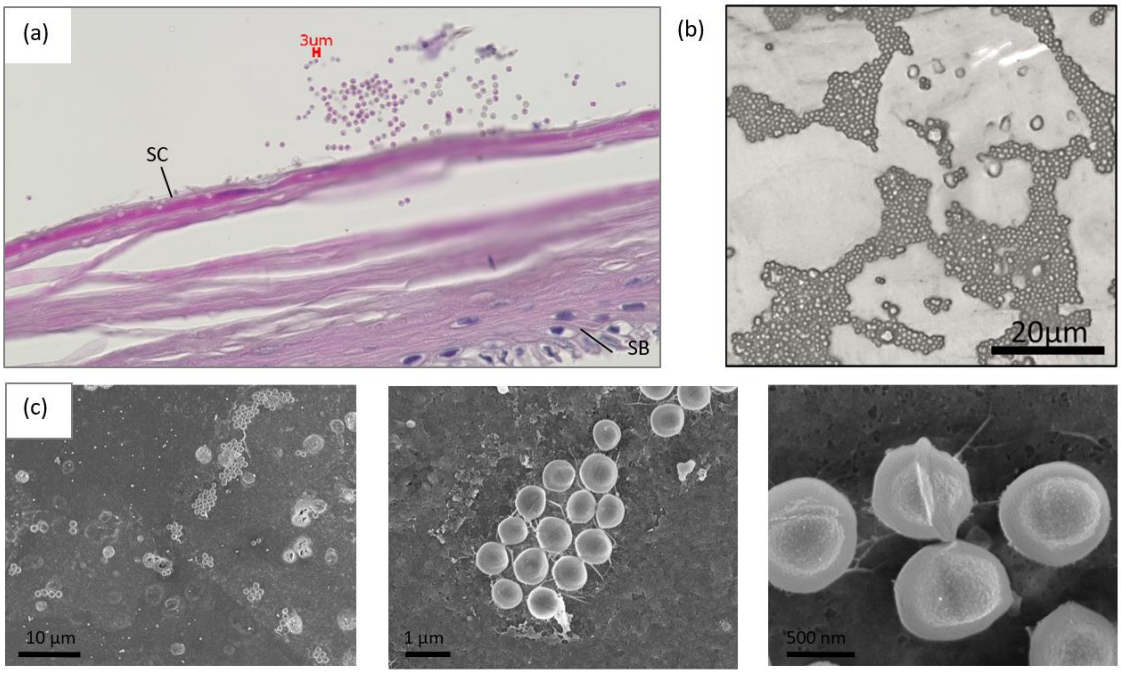

Figure 12: ***Staphylococcus colonisation on RHE model****: Staphylococcus epidermidis ATCC12228 were applied topically on the stratum corneum with PBS^- and incubated for 24 hours. (a) Haematoxylin-eosin staining of RHE models after addition of S. epidermidis. After microbial presence was confirmed in reflected-light microscopy (b) skin models were washed with PBS, fixed with glutardialdehyde (6%) and pictures were taken with scanning electron microscope (c). SC = Stratum corneum; SB = Stratum basale.*

5. Discussion

In this thesis different methods were explored to improve barrier function by modifying an existing protocol for RHE models. Multiple approaches stemming from existing literature and their respective conclusions were considered and tested using the barrier test method (see 3.2.1.) as it required less resources than an ET50 test. One approach involved manipulating calcium content within the media during ALI phase to simulate a wound situation and stimulate lamellar body formation and related repair mechanisms to compensate for the lacking barrier [51]. Unfortunately, initial results showed a poor response compared to the other approaches and it was abandoned (data not shown). In the discussion below, the other three approaches, GA treatment, LipidMix supplementation and the introduction of a human skin commensal are further elaborated.

5.1 Effects of glycolic acid treatment on the barrier function

This approach involved applying diluted glycolic acid ranging from 2%-10% for a peeling effect as it is a common practice for dermatologists [52]. It is also suggested that the elevated surface pH of RHE models may be a factor that impairs proper barrier formation and maintenance [53]. While it is not known whether an elevated surface pH is a causative or correlative factor of impaired barrier function, it was investigated if an artificial acidification of the surface would mitigate the defect. Unfortunately artificial acidification with GA consequently involved a more humid environment which has also been reported as a potential inhibitor of proper barrier formation [54]. The results obtained using the barrier test returned either an insignificant variance compared to untreated samples or a completely unviable RHE model when treated with less diluted acid ranging from 5% to 10%. A way to lower the surface pH without subjecting the RHE model to additional moisture would be preferable for future experiments. While the application of GA-containing water-in-oil emulsions has been applied to lower surface pH on in-vivo skin it may require additional adjustments and fine tuning to show this effect using in-vitro RHE models [55]. This would further support the hypothesis that hydrophilic properties of diluted GA may cancel out any positive effects on the barrier which have been reported in-vivo [52].

The H&E staining method highlights typical morphological structures to confirm proper formation of epidermal layers. This serves as an easily accessible qualitative control for RHE models as nonconformance stand out clearly when compared to controls. The apparent thickness of the SC appears to be misleading and not indicative of the barrier function. It is hypothesized that fixation and preparation of the sample slide produces a loose SC structure (see Fig. 4). A comparison between RHE treated with GA and standard protocol RHE doesn't reveal any notable differences while a desquamation effect is reported in literature [56]. This might be due to the lower concentration of GA in contrast to reported concentration. Unfortunately in regards to the barrier function this staining method seems to only provide limited information such as the amount of lamellar bodies found within the boundary of the SG. The decision to abandon this approach in favor of the LipidMix supplementation was made after the initial round of barrier test returned more promising results for the latter and no barrier function-enhancing effect was observed for the topical application of GA.

5.2 Effects of LipidMix supplementation on the barrier function

In this approach the culture media of the ALI phase was modified to contain additional FFA species by supplementing it with a defined lipid mixture from Sigma Aldrich. It is hypothesized that essential lipid species may be insufficient due to the missing dermal layer which would provide them in native human skin. This may alter lipids within the SC such as FFA chain length and desaturation status which have been reported to impact the barrier function negatively [37], [38], [51]. Initial experiments with lipid supplementation using the barrier test yielded increments of viability up to 20% compared to the control group (data not shown). Ultimately when tested using the ET50 test results were much more humbling with increments of viability varying from 4% to 10%. Such a discrepancy may explained by a gradual measure of variance over time when using the ET50 test in contrast to a single time point measurement after two hours in the barrier test. These result coincide with literature that reported that lipid supplementation affect the SC's lipid composition and hence it's barrier capability [51], [57]. To get a better understanding of how the LipidMix supplementation impacts the standard protocol, several different methods were used to characterize the changes

between these two RHE model protocols. As mentioned above the H&E staining method did not yield any satisfying results for the LipidMix supplemented models either (see Fig. 6). To further expand options in microscopy key enzymes and structural proteins were chosen to be visualized by immunohistochemistry. These proteins are known to play an important role in the formation and maintenance of the barrier functions. The structural proteins filaggrin, involucrin and ceramides were investigated. Filaggrin, a multi-functional 400 kDa protein, in its monomeric form is a degraded and dephosphorylated product of profilaggrin. It serves as intermediate filament between other structural proteins within the SC's extracellular matrix [58] and ultimately ends up being proteolyzed into amino acids contributing to the SC's acidic pH gradient. A filaggrin gene defect has been linked to skin diseases such as ichytosis vulgaris and other structural deficiencies like abnormal architecture of lamellar layers [59]. While not directly responsible for lipid processing, it has been suggested that filaggrin contributes to lamellar body loading and is known to be pivotal for proper barrier functions. Hence it serves as an additional control during immunohistochemistry experiments. A stronger signal in the LipidMix supplemented RHE models is observed when compared to the standard protocol which would suggest a stronger barrier. Ceramides are the focus point of this experiment, since they correspond up to 50% of the SC's lipids dry weight. Since the antibodies were IgM-type antibodies and their specificity to target a broad spectra of ceramide species, they also stain intracellular ceramides. Interestingly, there seems to be a difference between the signal distributions when comparing native tissue with either of the RHE models as the signal of the SC in the native tissue is stronger than in the RHE models. This might be a clue on the impaired barrier function and further highlights ceramides as an important marker concerning barrier function. Involucrin is a transglutaminase protein that functions as anchor between the CE and the lipid envelope, a monolayer of intercellular non-polar lipids [60], [61]. The signal of the antibody is stronger in the standard protocol RHE, but it is worthy to take note of the distribution of the signal. It seems to be stronger represented within the SC area of the LipidMix supplemented RHE model. According to literature Involucrin is bound by esterification mainly of its glutamate residue to omega-hydroxylated ceramide species or FFAs [62], [63]. It is hypothesized that once esterified and bound, the antibody might be hindered in its attachment and hence result in a

poor visibility in the SC. Lastly a rate-limiting enzyme called SCD1 was chosen [46]. As reported in literature the presences of SCD1 is altered when comparing RHE models with native human skin [37]. The SCD1 within the human skin is largely present within the SB as opposed to RHE models where a strong signal is detected in the differentiating layers. This was confirmed by the observations of the IHC pictures (See Figure 4.4). It is suggested by literature that the altered expression of SCD1 is linked to the increased amount of mono-unsaturated fatty acids within the SC lowering the barrier effect [37].

5.3 Further characterization utilizing non-invasive methods

Practical problems while developing new protocols for RHE include limited options for standardized test methods. Standardized methods such as OECD test guidelines for skin corrosion and skin irritation are invasive and result in destruction of cultured models. They also imply tissue fixation, labelling and destruction, which renders them unusable for further experiments. This restriction leads to experimental approaches yielding one-dimensional results while it is extremely helpful and important to able to assess results from multiple angles using the same batch of models.

One of these methods is called impedance spectroscopy. It is a non-invasive method to characterize the electrical resistance of cells, cell layers and tissues [64]. Using a sinusoidal current the resulting voltage between two electrodes is measured and the ohmic resistance can be derived. Parameters vary at each current frequency hence to avoid losing critical data it is necessary to measure and generate an impedance spectrum covering a range of frequencies [48]. It is suggested that a strong barrier function is associated with a high electrical resistance of the RHE skin model which is expressed in the output value, the TEER [48], [64]. A very interesting result was observed, since it went against the original expectation of LipidMix supplemented RHE models having a higher resistance. Instead no significant change was observed in two of the donors while the last one even showed the opposite effect of a lowered resistance after LipidMix supplementation. It is hypothesized that this effect could be a result of the SC’s lamellar lipids swelling due to the amount of increased lipid supplementation improving electrical flow by providing more surface of

hydrophilic head groups [65]. While this occurrence would not explain the variability of the impedance measurements it would not contradict the effect of improved resistance against irritative substances as seen in the ET50 and barrier test. It would be very interesting to assess the packing status of SC lipid as it is reported that skin models show a more loose hexagonal packing status in opposition to the more dense orthorhombic packing status of native human skin [36], [66], [67]. Further testing would be required for consistency within results to determine a definite effect.

Originating from the field of analytical chemistry Raman spectroscopy is a powerful non-invasive method to analyze the chemical composition of a complex tissue sample based on capturing inelastic scattering of a monochromatic laser [68]. During recent years it has also been extensively used to analyze biological data and generated a list of wavenumbers associated with bio-relevant chemical substances [43]. It is reported that Raman spectroscopy has been used to study the organization of SC lipid's intra- and inter-chain structure depending on the spectral range [50]. In this study the focus is the lateral packing state of the SC lipids which is reflected by methylene scissoring vibrational peaks detected within the 1050-1140 cm^{-1} region. The formular $S_{1130+1060}/S_{1080}$ has been used to calculate the ratio of trans-gauche conformers inside the acyl chains of the SC lipids. High values indicated a more compact lipid packing state while decreasing values are associated with more loose states [49]. While the use of the Raman spectroscopy covers considerably large amounts of data, for this study the focus was directed to 3 specific wavelengths corresponding to lateral packing states within lamellar lipids as suggested by [50]. These wavenumbers are 3 peaks within the spectrum range of 1030 nm^{-1} and 1130 nm^{-1} associated with trans-gauche conformers of acyl chains and the resulting ratio describes degree of closeness within lamellar lipids as mentioned above. During the first measurement of donor 15-017, values from the standard protocol suggest a tighter packing state than RHE models supplemented with LipidMix. This spectral data reflects similarity when compared with data obtained from impedance spectroscopy which reinforces the hypothesis of increased lipid amounts resulting in local swelling. This would disturb the orthorhombic structure lamellar lipids which is considered the tightest packing state [49]. Unfortunately this effect was not observed at the following iteration of this experiment when measuring

RHE models derived from donor 15-012 where the signals showed no significant difference in-between the protocols.

Methods to directly compare RHE models to in-vivo human skin are scarce. While finding new methods is one way to tackle the problem modifying old established methods is by no means inferior. TEWL has been extensively used by dermatologists to measure barrier function and diagnose skin health [69], [70] [71]. A simple adapter designed via CAD software SOLIDworks™ enabled the measurements of RHE models as it was not possible to directly use the probe on the SC surface as per instruction. The additional distance between electrodes and SC surface had to be factored into the calculation results using the formular kindly provided by the company Courage-Khazaka electronic (see Fig 11b). Multiple possibilities to measure RHE models were proposed but ultimately a consistent way of measuring the models within the 6-well culture well including E3 media underneath to simulate body fluids was chosen. When compared to the standard protocol the LipidMix supplemented RHE models show a decrease of TEWL values which indicate a higher difficulty for water molecules to pass through the model. When compensated for the additional distance the TEWL value even drops from a 16 g/h/m² value range to a 12-13 g/h/m² value range. Albeit still bad this result would be within acceptable boundaries for native human skin [72]. It is important to validate observed results in the future through further investigation.

It has to be considered if the response to LipidMix supplementation is variable depending either on the health condition or genetic disposition of the donor. Unfortunately, due to the origin of donor cells this cannot be easily determined as the donation agreement implies a strict discretion.

5.4 RHE models as models for bacterial colonization

In-vitro skin models are an attractive alternative especially when working with pathogenic species of microbes [73], [74]. However it is the opportunistic commensals which accompany humans through their everyday life that are most likely to have the biggest impact on the human skin [75], [16]. While exploring methods for bacterial colonization on the surfaces of RHE models *S. epidermidis*, a non-pathogenic native human skin inhabitant was chosen for testing. Bacterial

growth was observed even with antibiotics present within the cell culture media. Acquiring quantitative data was problematic as CFU counts on streaking plates relied on reliable and consistent extraction of bacterial populations from RHE models. The complete homogenization of RHE models colonized with *S. epidermidis* produced insignificant data with high variance which could not be evaluated (data not shown). Another problem which was identified after initial efforts to detect *S. epidermidis* using microscopy was the unwillingness of *S. epidermidis* to adhere to the SC's surface. This behavior changed after substituting the media on which the bacteria was initially applied from the ONC's full media for nutrient-deficient PBS^- as it is also suggested by the literature [76]. After this change *S. epidermidis* was observed adhering on the skin surface on a consistent basis (see Fig. 12c). The next step would be to observe bacterial growth on RHE models and investigate their impact both on surface acidity and barrier function. It is also noteworthy that natural environmental conditions on native human skin are not as humid as cell culture conditions as it has been pointed out [77]. While in this thesis the primary focus was to investigate a potential effect of microbial commensals on the skin barrier function, it would also contribute to possibilities of in-vitro models serving as models for future infection studies [74], [78].

5.5 Outlook

Although improvement, which suggest a better barrier function, have been achieved, the results also imply that much work has still to be done to achieve a consistent and ubiquitous effect across results of different measurement methods. The LipidMix components include a range of various fatty acids and while some of them had their expression and mechanics investigated, it is still largely an enigma of intricate regulation systems that supplies the native human skin with an optimal amount and ratio of lipid species [37], [51]. The approaches taken in this thesis were but a few suggestions within literature to try and solve the deficiency in barrier function within the current RHE models. A few other interesting approaches include the manipulation of air humidity during the ALI phase which was shown to be in proportionally correlated to the barrier function [54]. The higher the humidity, the lower the barrier function. Unfortunately, it is

not easy to manipulate air humidity within incubators without facing the challenge of evaporating culture media. It would easily incur disastrous consequences of a depriving RHEs of media. Other research groups have published data that suggest an altered expression of enzymes like SCD1 as mentioned above which resulted in abnormal ratios of lipid species such as mono-unsaturated fatty acids (MUFA) or sphingomyelin/ceramides [37], [79]. Although no clear causative relation is established yet they provide important clues for future approaches engaging this topic. On the other hand the concept of skin commensals and their interaction with in-vitro RHE models is yet to be fully explored. Literature shows that these bacterial cohabitants of the human skin contribute enough to warrant investigation on RHE in the future.

References

[1] J. A. Sanford and R. L. Gallo, “Functions of the skin microbiota in health and disease.,” *Semin. Immunol.*, vol. 25, no. 5, pp. 370–7, Nov. 2013.

[2] T. Welss, D. A. Basketter, and K. R. Schröder, “In vitro skin irritation: facts and future. State of the art review of mechanisms and models.,” *Toxicol. In Vitro*, vol. 18, no. 3, pp. 231–43, Jun. 2004.

[3] K. R. Feingold, “The outer frontier: the importance of lipid metabolism in the skin.,” *J. Lipid Res.*, vol. 50 Suppl, pp. S417–S422, 2009.

[4] J. Van Smeden, M. Janssens, G. S. Gooris, and J. a. Bouwstra, “The important role of stratum corneum lipids for the cutaneous barrier function,” *Biochim. Biophys. Acta - Mol. Cell Biol. Lipids*, vol. 1841, no. 3, pp. 295–313, 2014.

[5] P. M. Elias, M. L. Williams, E. H. Choi, and K. R. Feingold, “Role of cholesterol sulfate in epidermal structure and function: Lessons from X-linked ichthyosis,” *Biochim. Biophys. Acta - Mol. Cell Biol. Lipids*, vol. 1841, no. 3, pp. 353–361, 2014.

[6] A. S. Michaels, S. K. Chandrasekaran, and J. E. Shaw, “Drug permeation through human skin: Theory andinvitro experimental measurement,” *AIChE J.*, vol. 21, no. 5, pp. 985–996, Sep. 1975.

[7] P. M. Elias and E. H. Choi, “Interactions among stratum corneum defensive functions.,” *Exp. Dermatol.*, vol. 14, no. 10, pp. 719–26, Oct. 2005.

[8] K. R. Feingold, M. Schmuth, and P. M. Elias, “The Regulation of Permeability Barrier Homeostasis,” *J. Invest. Dermatol.*, vol. 127, no. 7, pp. 1574–1576, 2007.

[9] P. M. Elias and K. R. Feingold, *Skin Barrier*, vol. 1. 2006.

[10] M. Fartasch, “The Epidermal Lamellar Body as a Multifunctional Secretory Organelle,” in *Skin Barrier*, CRC Press, 2005, pp. 261–272.

[11] M. Mao-Qiang, K. R. Feingold, M. Jain, and P. M. Elias, “Extracellular processing of phospholipids is required for permeability barrier homeostasis.,” *J. Lipid Res.*, vol. 36, no. 9, pp. 1925–35, 1995.

[12] M. Mao-Qiang, M. Jain, K. R. Feingold, and P. M. Elias, “Secretory phospholipase A2 activity is required for permeability barrier homeostasis,” *J Invest Dermatol*, vol. 106, no. 1, pp. 57–63, 1996.

[13] J. M. Jensen, S. Schütze, M. Förl, M. Krönke, and E. Proksch, “Roles for tumor necrosis factor receptor p55 and sphingomyelinase in repairing the cutaneous permeability barrier,” *J. Clin. Invest.*, vol. 104, no. 12, pp. 1761–1770, 1999.

[14] M. Schmuth, M. Q. Man, F. Weber, W. Gao, K. R. Feingold, P. Fritsch, P. M. Elias, and W. M. Holleran, “Permeability barrier disorder in Niemann-Pick disease: Sphingomyelin-ceramide processing required for normal barrier homeostasis,” *J. Invest. Dermatol.*, vol. 115, no. 3, pp. 459–466, 2000.

[15] J. P. Leeming, K. T. Holland, and W. J. Cunliffe, “The microbial ecology of pilosebaceous units isolated from human skin.,” *J. Gen. Microbiol.*, vol. 130, no. 4, pp. 803–7, Apr. 1984.

[16] E. A. Grice and J. A. Segre, “The skin microbiome,” *Nat. Rev. Microbiol.*, vol. 9, no. 4, pp. 244–253, Apr. 2011.

[17] H. Lambers, S. Piessens, A. Bloem, H. Pronk, and P. Finkel, “Natural skin surface pH is on average below 5, which is beneficial for its resident flora,” *Int. J. Cosmet. Sci.*, vol. 28, no. 5, pp. 359–370, 2006.

[18] W. C. Noble, “The human skin microflora and disease,” in *Medical Importance of the Normal Microflora*, G. W. Tannock, Ed. Boston, MA: Springer US, 1999, pp. 24–46.

[19] K. Holland, “Cosmetics, what is their influence on skin microflora?,” *Am. J. Clin. Dermatol.*, vol. 3, pp. 455–459, 2002.

[20] C. S. Weil and R. A. Scala, “Study of intra- and interlaboratory variability in the results of rabbit eye and skin irritation tests,” *Toxicol. Appl. Pharmacol.*, vol. 19, no. 2, pp. 276–360, 1971.

[21] J. H. DRAIZE, G. WOODARD, and H. O. CALVERY, “METHODS FOR THE STUDY OF IRRITATION AND TOXICITY OF SUBSTANCES APPLIED TOPICALLY TO THE SKIN AND MUCOUS MEMBRANES,” *J. Pharmacol. Exp. Ther.*, vol. 82, no. 3, 1944.

[22] W. M. Russell, R. L. Burch, and C. W. Hume, *Principles of Human Experimental Technique*. 1957.

[23] “Commission Staff Working document, Timetables for the phasing-out of animal testing in the framework of the 7th Amendment to the Cosmetics Directive (Council Directive 76/768/EEC), Register for commission documents SEC(2004) 1210.” 2004.

[24] T. Hartung, S. Bremer, S. Casati, S. Coecke, R. Corvi, S. Fortaner, L. Gribaldo, M. Halder, A. J. Roi, P. Prieto, E. Sabbioni, A. Worth, and V. Zuang, “ECVAM’s Response to the Changing Political Environment for Alternatives: Consequences of the European Union Chemicals and Cosmetics Policies,” *ATLA Altern. to Lab. Anim.*, vol. 31, no. 5, pp. 473–481, 2003.

[25] “Regulation (EC) No 1907/2006 of the European Parliament and of the Council of 18 December 2006 concerning the Registration, Evaluation, Authorisation and Restriction of Chemicals (REACH), establishing a European Chemicals Agency.” .

[26] J. G. Hengstler, H. Foth, R. Kahl, P.-J. Kramer, W. Lilienblum, T. Schulz, and H. Schweinfurth, “The REACH concept and its impact on toxicological sciences.,” *Toxicology*, vol. 220, no. 2–3, pp. 232–9, Mar. 2006.

[27] H. Breithaupt, “The costs of REACH. REACH is largely welcomed, but the requirement to test existing chemicals for adverse effects is not good news for all.,” *EMBO Rep.*, vol. 7, no. 10, pp. 968–71, Oct. 2006.

[28] A. El Ghalbzouri, R. Siamari, R. Willemze, and M. Ponec, “Leiden reconstructed human epidermal model as a tool for the evaluation of the skin corrosion and irritation potential according to the ECVAM guidelines,” *Toxicol. Vitr.*, vol. 22, no. 5, pp. 1311–1320, 2008.

[29] H. Kandárová, M. Liebsch, H. Spielmann, E. Genschow, E. Schmidt, D. Traue, R. Guest, A. Whittingham, N. Warren, A. O. Gamer, M. Remmele, T. Kaufmann, E. Wittmer, B. De Wever, and M. Rosdy, “Assessment of the human epidermis model SkinEthic RHE for in vitro skin corrosion testing of chemicals according to new OECD TG 431.,” *Toxicol. In Vitro*, vol. 20, no. 5, pp. 547–59, Aug. 2006.

[30] A. Coquette, N. Berna, A. Vandenbosch, M. Rosdy, B. De Wever, and Y. Poumay, “Analysis of interleukin-1alpha (IL-1alpha) and interleukin-8 (IL-8) expression and release in in vitro reconstructed human epidermis for the prediction of in vivo skin irritation and/or sensitization.,” *Toxicol. In Vitro*, vol. 17, no. 3, pp. 311–21, Jun. 2003.

[31] Y. Poumay, F. Dupont, S. Marcoux, M. Leclercq-Smekens, M. Hérin, and a. Coquette, “A simple reconstructed human epidermis: Preparation of the culture model and utilization in in vitro studies,” *Arch. Dermatol. Res.*, vol. 296, no. 5, pp. 203–211, 2004.

[32] J. N. Mansbridge, “Tissue-engineered skin substitutes in regenerative medicine.,” *Curr. Opin. Biotechnol.*, vol. 20, no. 5, pp. 563–7, Oct. 2009.

[33] G. T. Park, E. Y. Seo, K. M. Lee, D. Y. Lee, and J. M. Yang, “Tob is a potential marker gene for the basal layer of the epidermis and is stably expressed in human primary keratinocytes.,” *Br. J. Dermatol.*, vol. 154, no. 3, pp. 411–8, Mar. 2006.

[34] R. Bajpai, J. Lesperance, M. Kim, and A. V Terskikh, “Efficient propagation of single cells Accutase-dissociated human embryonic stem cells.,” *Mol. Reprod. Dev.*, vol. 75, no. 5, pp. 818–27, May 2008.

[35] M. Pruniéras, M. Régnier, and D. Woodley, “Methods for cultivation of keratinocytes with an air-liquid interface.,” *J. Invest. Dermatol.*, vol. 81, no.

1 Suppl, p. 28s–33s, Jul. 1983.

[36] V. S. Thakoersing, G. S. Gooris, A. Mulder, M. Rietveld, A. El Ghalbzouri, and J. a. Bouwstra, “Unraveling Barrier Properties of Three Different In-House Human Skin Equivalents,” *Tissue Eng. Part C Methods*, vol. 18, no. 1, pp. 1–11, 2012.

[37] V. S. Thakoersing, J. van Smeden, A. a Mulder, R. J. Vreeken, A. El Ghalbzouri, and J. a Bouwstra, “Increased Presence of Monounsaturated Fatty Acids in the Stratum Corneum of Human Skin Equivalents,” *J. Invest. Dermatol.*, vol. 133, no. 1, pp. 59–67, 2012.

[38] K. R. Feingold and P. M. Elias, “Role of lipids in the formation and maintenance of the cutaneous permeability barrier,” *Biochim. Biophys. Acta - Mol. Cell Biol. Lipids*, vol. 1841, no. 3, pp. 280–294, 2014.

[39] K. Richter, “Skin aging, gene expression and calcium,” *Exp. Gerontol.*, 2014.

[40] a V Rawlings and C. R. Harding, “Moisturization and skin barrier function,” *Dermatol.Ther.*, vol. 17 Suppl 1, no. 1396–0296 (Print), pp. 43–48, 2004.

[41] J. a Bouwstra, H. W. W. Groenink, J. a Kempenaar, S. G. Romeijn, and M. Ponec, “Water distribution and natural moisturizer factor content in human skin equivalents are regulated by environmental relative humidity.,” *J. Invest. Dermatol.*, vol. 128, no. 2, pp. 378–388, 2008.

[42] O. Arqués, I. Chicote, S. Tenbaum, I. Puig, and H. G. Palmer, “Standardized Relative Quantification of Immunofluorescence Tissue Staining,” *Protoc. Exch.*, 2012.

[43] A. C. S. Talari, Z. Movasaghi, S. Rehman, and I. ur Rehman, “Raman Spectroscopy of Biological Tissues,” *Appl. Spectrosc. Rev.*, vol. 50, no. 1, pp. 46–111, 2015.

[44] S. J. Brown and W. H. I. McLean, “One remarkable molecule: filaggrin.,” *J. Invest. Dermatol.*, vol. 132, no. 3 Pt 2, pp. 751–62, Mar. 2012.

[45] M. B. Yaffe, S. Murthy, and R. L. Eckert, “Evidence that involucrin is a covalently linked constituent of highly purified cultured keratinocyte cornified envelopes.,” *J. Invest. Dermatol.*, vol. 100, no. 1, pp. 3–9, Jan. 1993.

[46] J. M. Ntambi and M. Miyazaki, “Regulation of stearoyl-CoA desaturases and role in metabolism.,” *Prog. Lipid Res.*, vol. 43, no. 2, pp. 91–104, Mar. 2004.

[47] Y. Masukawa, H. Narita, H. Sato, A. Naoe, N. Kondo, Y. Sugai, T. Oba, R. Homma, J. Ishikawa, Y. Takagi, and T. Kitahara, “Comprehensive quantification of ceramide species in human stratum corneum.,” *J. Lipid Res.*, vol. 50, no. 8, pp. 1708–1719, 2009.

[48] F. Groeber, L. Engelhardt, S. Egger, H. Werthmann, M. Monaghan, H. Walles, and J. Hansmann, “Impedance Spectroscopy for the Non-Destructive Evaluation\rof In Vitro Epidermal Models,” *Pharm Res*, vol. 32, pp. 1845–1854, 2015.

[49] A. Tfayli, E. Guillard, M. Manfait, and A. Baillet-Guffroy, “Thermal dependence of Raman descriptors of ceramides. Part I: Effect of double bonds in hydrocarbon chains,” *Anal. Bioanal. Chem.*, vol. 397, no. 3, pp. 1281–1296, 2010.

[50] A. Quatela, A. Tfayli, and A. Baillet-Guffroy, “Examination of the effect of Stratum Corneum isolation process on the integrity of the barrier function: A confocal Raman spectroscopy study,” *Ski. Res. Technol.*, vol. 22, no. 1, pp. 75–80, 2016.

[51] P. M. Elias, R. Gruber, D. Crumrine, G. Menon, M. L. Williams, J. S. Wakefield, W. M. Holleran, and Y. Uchida, “Formation and functions of the corneocyte lipid envelope (CLE),” *Biochim. Biophys. Acta - Mol. Cell Biol. Lipids*, vol. 1841, no. 3, pp. 314–318, 2014.

[52] J. Sharad, “Glycolic acid peel therapy - a current review.,” *Clin. Cosmet. Investig. Dermatol.*, vol. 6, pp. 281–8, 2013.

[53] M. J. Behne, N. P. Barry, K. M. Hanson, I. Aronchik, R. W. Clegg, E. Gratton, K. Feingold, W. M. Holleran, P. M. Elias, and T. M. Mauro, “Neonatal development of the stratum corneum pH gradient: Localization and mechanisms leading to emergence of optimal barrier function,” *J. Invest. Dermatol.*, vol. 120, no. 6, pp. 998–1006, 2003.

[54] M. Denda, J. Sato, Y. Masuda, T. Tsuchiya, J. Koyama, M. Kuramoto, P. M. Elias, and K. R. Feingold, “Exposure to a dry environment enhances epidermal permeability barrier function,” *J. Invest. Dermatol.*, vol. 111, no. 5, pp. 858–863, 1998.

[55] B. Behm, M. Kemper, P. Babilas, C. Abels, and S. Schreml, “Impact of a Glycolic Acid-Containing pH 4 Water-in-Oil Emulsion on Skin pH,” *Skin Pharmacol. Physiol.*, vol. 28, no. 6, pp. 290–295, 2015.

[56] M. Fartasch, J. Teal, and G. K. Menon, “Mode of action of glycolic acid on human stratum corneum: Ultrastructural and functional evaluation of the epidermal barrier,” *Arch. Dermatol. Res.*, vol. 289, no. 7, pp. 404–409, 1997.

[57] V. S. Thakoersing, J. van Smeden, W. A. Boiten, G. S. Gooris, A. A. Mulder, R. J. Vreeken, A. El Ghalbzouri, and J. A. Bouwstra, “Modulation of stratum corneum lipid composition and organization of human skin equivalents by specific medium supplements.,” *Exp. Dermatol.*, vol. 24, no. 9, pp. 669–74, Sep. 2015.

[58] M. Manabe, M. Sanchez, T.-T. Sun, and B. A. Dale, “Interaction of filaggrin with keratin filaments during advanced stages of normal human epidermal differentiation and in Ichthyosis vulgaris,” *Differentiation*, vol. 48, no. 1, pp. 43–50, 1991.

[59] R. Gruber, P. M. Elias, D. Crumrine, T. K. Lin, J. M. Brandner, J. P. Hachem, R. B. Presland, P. Fleckman, A. R. Janecke, A. Sandilands, W. H. I. McLean, P. O. Fritsch, M. Mildner, E. Tschachler, and M. Schmuth, “Filaggrin genotype in ichthyosis vulgaris predicts abnormalities in epidermal structure and function,” *Am. J. Pathol.*, vol. 178, no. 5, pp. 2252–

2263, 2011.

[60] Z. Nemes, L. N. Marekov, L. Fésüs, and P. M. Steinert, “A novel function for transglutaminase 1: attachment of long-chain omega-hydroxyceramides to involucrin by ester bond formation.,” *Proc. Natl. Acad. Sci. U. S. A.*, vol. 96, no. 15, pp. 8402–8407, 1999.

[61] M. Behne, Y. Uchida, T. Seki, P. Ortiz De Montellano, P. M. Elias, and W. M. Holleran, “Omega-hydroxyceramides are required for corneocyte lipid envelope (CLE) formation and normal epidermal permeability barrier function,” *J. Invest. Dermatol.*, vol. 114, no. 1, pp. 185–192, 2000.

[62] N. D. Lazo, J. G. Meine, and D. T. Downing, “Lipids are covalently attached to rigid corneocyte protein envelopes existing predominantly as beta-sheets: a solid-state nuclear magnetic resonance study.,” *J. Invest. Dermatol.*, vol. 105, no. 2, pp. 296–300, Aug. 1995.

[63] L. N. Marekov and P. M. Steinert, “Ceramides Are Bound to Structural Proteins of the Human Foreskin Epidermal Cornified Cell Envelope,” *J. Biol. Chem.*, vol. 273, no. 28, pp. 17763–17770, Jul. 1998.

[64] U. Birgersson, E. Birgersson, P. Aberg, I. Nicander, and S. Ollmar, “Non-invasive bioimpedance of intact skin: mathematical modeling and experiments.,” *Physiol. Meas.*, vol. 32, no. 1, pp. 1–18, 2011.

[65] C. Pichonnaz, J.-P. Bassin, E. Lécureux, D. Currat, and B. M. Jolles, “Bioimpedance spectroscopy for swelling evaluation following total knee arthroplasty: a validation study.,” *BMC Musculoskelet. Disord.*, vol. 16, p. 100, 2015.

[66] J. A. Bouwstra, G. S. Gooris, F. E. Dubbelaar, and M. Ponec, “Phase behavior of lipid mixtures based on human ceramides: coexistence of crystalline and liquid phases.,” *J. Lipid Res.*, vol. 42, no. 11, pp. 1759–70, Nov. 2001.

[67] F. Damien and M. Boncheva, “The extent of orthorhombic lipid phases in the stratum corneum determines the barrier efficiency of human skin in

vivo.," *J. Invest. Dermatol.*, vol. 130, no. 2, pp. 611–4, Feb. 2010.

[68] M. Steinke, R. Gross, H. Walles, R. Gangnus, K. Schütze, and T. Walles, "An engineered 3D human airway mucosa model based on an SIS scaffold," *Biomaterials*, vol. 35, no. 26, pp. 7355–7362, 2014.

[69] K. V Roskos and R. H. Guy, "Assessment of skin barrier function using transepidermal water loss: effect of age.," *Pharm. Res.*, vol. 6, no. 11, pp. 949–53, Nov. 1989.

[70] M. Kelleher, A. Dunn-Galvin, J. O. Hourihane, D. Murray, L. E. Campbell, W. H. I. McLean, and A. D. Irvine, "Skin barrier dysfunction measured by transepidermal water loss at 2 days and 2 months predates and predicts atopic dermatitis at 1 year.," *J. Allergy Clin. Immunol.*, vol. 135, no. 4, p. 930–5.e1, Apr. 2015.

[71] F. Gioia and L. Celleno, "The dynamics of transepidermal water loss (TEWL) from hydrated skin.," *Skin Res. Technol.*, vol. 8, no. 3, pp. 178–86, Aug. 2002.

[72] J. du Plessis, A. Stefaniak, F. Eloff, S. John, T. Agner, T.-C. Chou, R. Nixon, M. Steiner, A. Franken, I. Kudla, and L. Holness, "International guidelines for the in vivo assessment of skin properties in non-clinical settings: Part 2. transepidermal water loss and skin hydration.," *Skin Res. Technol.*, vol. 19, no. 3, pp. 265–78, Aug. 2013.

[73] L. Popov, J. Kovalski, G. Grandi, F. Bagnoli, and M. R. Amieva, "Three-dimensional human skin models to understand Staphylococcus aureus skin colonization and infection," *Front. Immunol.*, vol. 5, no. FEB, pp. 1–6, 2014.

[74] J. Shepherd, I. Douglas, S. Rimmer, L. Swanson, and S. MacNeil, "Development of three-dimensional tissue-engineered models of bacterial infected human skin wounds.," *Tissue Eng. Part C. Methods*, vol. 15, no. 3, pp. 475–484, 2009.

[75] A. L. Cogen, V. Nizet, and R. L. Gallo, "Skin microbiota: A source of disease or defence?," *Br. J. Dermatol.*, vol. 158, no. 3, pp. 442–455, 2008.

[76] G. Lerebour, S. Cupferman, and M. N. Bellon-Fontaine, “Adhesion of Staphylococcus aureus and Staphylococcus epidermidis to the Episkin?? reconstructed epidermis model and to an inert 304 stainless steel substrate,” *J. Appl. Microbiol.*, vol. 97, no. 1, pp. 7–16, 2004.

[77] D. B. Holland, R. A. Bojar, A. H. T. Jeremy, E. Ingham, and K. T. Holland, “Microbial colonization of an in vitro model of a tissue engineered human skin equivalent--a novel approach.,” *FEMS Microbiol. Lett.*, vol. 279, no. 1, pp. 110–5, Feb. 2008.

[78] T. Bhattacharyya, M. Edward, C. Cordery, and M. D. Richardson, “Colonization of living skin equivalents by *Malassezia furfur*,” *Med. Mycol.*, vol. 36, no. 1, pp. 15–19, Jan. 1998.

[79] P. Pullmannová, K. Staňková, M. Pospíšilová, B. Školová, J. Zbytovská, and K. Vávrová, “Effects of sphingomyelin/ceramide ratio on the permeability and microstructure of model stratum corneum lipid membranes,” *Biochim. Biophys. Acta - Biomembr.*, vol. 1838, no. 8, pp. 2115–2126, 2014.

Image index

List of tables

List of abbreviations

3D	Three-dimensional
ALI	Air-liquid interface
ANOVA	Analysis of variance
CAD	Computer-assisted design
CE	Cornified envelope
CFU	Colony forming unit
DAPI	4',6-Diamidino-2-phenylindole dihydrochloride
DI	Deionized
DMSO	Dimethyl sulfoxide
DNA	Deoxyribonucleic acid
ECVAM	European Centre for the Validation of Alternative Methods
EDTA	Ethylenediaminetetaacetic acid
EU	European Union
FCS	Fetal calf serum
FFA	Free fatty acids
GA	Glycolic acid
H&E	haematoxylin and eosin
HEK	Human epidermal keratinocytes
HKGS	Human keratinocyte growth supplement
IHC	Immunohistochemistry
IMIB	Institute for Molecular Infection Biology
KGF	Keratinocyte growth factor
MTT	3-(4,5-Dimethylthiazol-2-yl)-2,5diphenyltetrazolium bromide
MUFA	Mono-unsaturated fatty acids
OD	optical density

OECD	Organisation for Economic Co-operation and Development	6
ONC	Overnight culture	21
PBS	Phosphate-buffered saline	9
PCM	Polycarbonate membrane	24
REACH	Regulation, Evaluation, Authorisation and Restriction of Chemicals	5
RHE	Reconstructed human epidermis	6
SB	Stratum basale	2
SC	Stratum corneum	2
SCD1	Stearyl-CoA desaturase-1	29
SEM	Scanning electron microscope	22
SG	Stratum granulosum	2
SS	Stratum spinosum	2
TEER	Transepithelial electrical resistance	31
TEWL	Transepidermal waterloss	20
TG	Test guideline	6
TS	Tryptic soy	9
UV	Ultraviolet	1